New odonatans (Odonata: Gomphaeschnidae; Synlestidae) from the Paleocene Paskapoo Formation: systematic and biogeographical implications

Corentin Jouault, Baptiste Coutret, Kurt O. Konhauser & André Nel

   View supplementary material

   Published online: 20 Nov 2023.

   Submit your article to this journal

   View related articles

   View Crossmark data
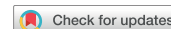
Taylor & Francis
Taylor & Francis Group

Check for updates

New odonatans (Odonata: Gomphaeschnidae; Synlestidae) from the Paleocene Paskapoo Formation: systematic and biogeographical implications

Corentin Jouault[a,b,c,d]* (iD), Baptiste Coutret[d] (iD), Kurt O. Konhauser[d] (iD) and André Nel[a] (iD)

[a]*Institut de Systématique, Évolution, Biodiversité (ISYEB), UMR 7205, Muséum National d'Histoire Naturelle, CNRS, Sorbonne Université, EPHE, Université Des Antilles, CP50, 57 rue Cuvier, F-75005 Paris, France;* [b]*Géosciences Rennes (UMR 6118), Université de Rennes, CNRS, F-35000 Rennes, France;* [c]*Institut des Sciences de l'Évolution (UMR 5554), Université de Montpellier, CNRS, F-34095 Montpellier, France;* [d]*Department of Earth and Atmospheric Sciences, University of Alberta, Edmonton, AB, T6G 2E3, Canada*

The Paleocene Paskapoo Formation in Alberta, Canada, offers a unique opportunity to gain insight into insect diversity at that time. This fossil insect-rich formation has yielded a variety of fossil arthropod specimens, including several wings of Odonata related to the genus *Alloaeschna* Wighton and Wilson, 1986. Here, we demonstrate that morphological characters previously used to separate three species are instead the result of intraspecific variability. We reinforce this demonstration using two examples of high variability and plasticity in modern species of the family Aeshnidae. Accordingly, we reinterpreted the taxonomic position of *Alloaeschna marklae* Wighton and Wilson, 1986 syn. nov. and *Alloaeschna quadrata* Wighton and Wilson, 1986 syn. nov. as junior synonyms of *Alloaeschna paskapooensis* Wighton and Wilson, 1986. In addition, we describe the first occurrence of a zygopteran in the Paskapoo Formation, namely *Albertalestes paskapooensis* gen. et sp. nov. (Synlestidae). Importantly, this new taxon is the first representative of the family found in North America. We also reconstructed the relationships within the Synlestidae under Bayesian inferences with a newly assembled matrix. Finally, we discuss the biogeography of the clade considering its fossil record using parsimony ancestral state reconstruction.

http://zoobank.org/urn:lsid:zoobank.org:pub:D5282228-2D59-46E9-B712-3DC5A71C42FD

Keywords: Insecta; Odonatoptera; Zygoptera; Lestiformia; palaeodiversity

Introduction

The Paleocene Epoch (66–56 Ma) is a key time in the evolutionary history of insect lineages because it encompasses a period of gradual warming (lasting *c.* 6 Ma) and ends with a thermal optimum (Paleocene–Eocene Thermal Maximum, or PETM) (e.g. Zachos et al., 2008). These global climate changes (variations in warming and cooling periods) are presumably drivers of the diversity dynamics of insect populations (e.g. Condamine et al., 2016; Halsch et al., 2021). In fact, these climate changes may have directly affected the insect's food sources – notably the gymnosperms (e.g. Condamine et al., 2020) – or their environment by reshaping the distribution of biomes (e.g. Korasidis et al., 2022). For instance, it has been recently demonstrated that the global warming of the Paleocene led to a worldwide modification of biome repartitioning and to the extension of temperate climates to high latitudes (e.g. Jouault et al., 2021; Korasidis et al., 2022). As a result, insects may have colonized new habitats, declined in former habitats, or persisted and dispersed.

To understand how these changes shaped the repartition of insects it is important to study their biogeographical history. This can be done by studying their fossil record and documenting new lineages and/or by reconstructing the phylogenetic relationships between species (e.g. Crisp et al., 2011). The fossil record allows us to document worldwide distributions in the past even though their current distribution is relict and restrained to a small area (Barden & Ware, 2017; Coiro et al., 2023). Similarly, the study of the relationships between extant species often provides clues on the 'ancestral' distribution of the clade and their evolutionary history. However, a patchy fossil record as well as a reduced sampling of the extant diversity – when relict from a flourishing diversity in the fossil record – can hamper these approaches.

Fortunately, some insect orders, such as the Odonata (i.e. dragonflies and damselflies), are often fossilized in lacustrine palaeoenvironments, thereby making it possible to accurately track their evolution (Bechly et al., 2001; Fleck et al., 1999; Nel, 2021; Nel et al., 2010; Vassilenko, 2014; Zheng, 2022). It has been demonstrated that numerous

---

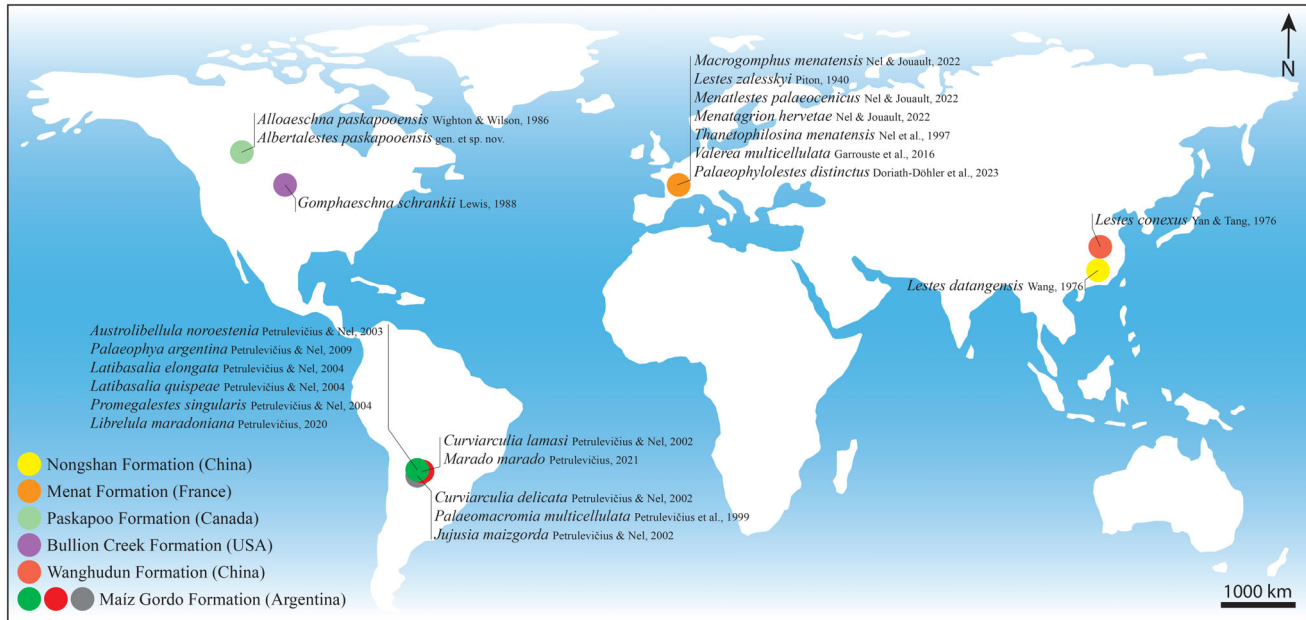*Corresponding author. Email: jouaultc0@gmail.com

Figure 1. Distribution of Paleocene odonatans plotted on a map of the Earth in its present configuration (modified after Jouault et al., 2020). **Abbreviations: N,** North; **km,** kilometers.

extant odonatan lineages arose during the Cretaceous and Paleocene (Kohli et al., 2021; Suvorov et al., 2022), which correlates well with their diversity during this time interval (about 20 Odonata species are known during the Paleocene: Fig. 1). Interestingly, some Paleocene deposits are still poorly studied, even though several odonatans have been described and new materials have been collected. This is the case for the Paskapoo Formation in Alberta (Canada), which has yielded well-preserved odonatan specimens. We use these specimens to reinterpret the limits of three species of *Alloaeschna* Wighton and Wilson, 1986. Among the new material, we found a well-preserved wing of the family Synlestidae, which informs the distribution of the family during the Paleocene and reduces the gaps in the synlestid fossil record.

The oldest records of Synlestidae are dated to the Cretaceous (Huang et al., 2022; Vasilenko, 2005). Recently, the phylogenetic relationships between extant representatives of the family were explored using molecular data and a maximum likelihood approach (Simaika et al., 2020). This study also discussed the biogeography of the clade and suggested a single African origin in the Synlestidae (Simaika et al., 2020). We propose new phylogenetic analyses of the extant Synlestidae using Bayesian inferences and molecular data. To reconstruct these new phylogenies, we applied additional genetic loci (five vs two) and reduced the number of terminal taxa. The reduction of the taxonomic sampling maximizes the completeness of our data set. Based on the resulting consensus trees we discuss

the biogeography of the family Synlestidae considering its fossil record.

Material and methods

Taxonomic sampling and alignment

All DNA sequences were retrieved from data available on GenBank (https://www.ncbi.nlm.nih.gov/genbank). Genes were selected to include coding and non-coding fragments and were extracted for five loci for 10 Synlestidae species and six outgroup taxa belonging to the families Lestidae, Perilestidae and Hemiphlebiidae. The five genetic loci are identified as follows: 16S ribosomal RNA (16S), 18S ribosomal RNA (18S), 28S ribosomal RNA (28S), Cytochrome Oxidase I (COI) and Cytochrome Oxidase II (COII). Wherever possible, sequences with the same voucher code were utilised to limit the use of chimeric taxa and avoid potential misidentification. To detect erroneous data, we BLASTed all the sequences and manually checked all the posterior alignments. The GenBank accession numbers are available in Supplemental material 1.

We aligned each locus individually using MAFFT v. 7.511 (Katoh & Standley, 2013) using the default settings and manually examined the resulting alignments to ensure that a fully codon-based alignment was generated, and examined coding frames and stop codons to detect potential pseudogenes or errors using Aliview v. 1.28 (Larsson, 2014). The final alignments for all five loci were concatenated into a single matrix using

SequenceMatrix v. 1.7.7 (Vaidya et al., 2011), with the external gaps recoded as question marks. The concatenated molecular matrix contains 16 taxa and 5832 sites (419 parsimony-informative, 370 singleton sites and 5043 constant sites) with 13.4% missing data. The alignment files are available in Supplemental material 2. We refrain from integrating fossil taxa into a total-evidence analysis (i.e. combining molecular and morphological data) because some fossil representatives of the family Synlestidae are known only from isolated wings. This partial preservation does not allow for coding numerous key morphological characters often used to delineate extant synlestid species.

Partitioning schemes and model selection

We used PartitionFinder v. 2.1.1 software (Lanfear et al., 2016) to determine suitable partitioning schemes and corresponding models of molecular evolution for the concatenated multiple sequence alignment generated in the previous step. We designated nine data blocks representing the three codon positions for each gene. Models were searched for MrBayes (*mrbayes*), the branch lengths set to *linked*, a Bayesian information criterion option (*BIC*) used for model selection and comparison, and a greedy algorithm used for schemes search (*greedy*). PartitionFinder determined six subsets from the nine data blocks (Supplemental material Table 1).

Phylogenetic analyses

Bayesian analyses were run in MrBayes v. 3.2.7 (Huelsenbeck & Ronquist, 2001; Ronquist & Huelsenbeck, 2003; Ronquist et al., 2012) under the models specified by PartitionFinder for molecular data. We also ran an analysis without substitution models selected *a priori* using reversible jump Markov chain Monte Carlo (rjMCMC) in MrBayes. This approach samples the posterior probability of all models in the GTR substitution family (Huelsenbeck et al., 2004). For the other parameters, we used the default parametrization. *Hemiphlebia mirabilis* was used as outgroup and the monophyly of the Synlestidae was constrained. All analyses comprised two runs and four chains and were launched for 20 million generations. Chains were sampled every 5000 generations and a burn-in fraction of 0.25 was used. Convergence diagnostics were checked for each analysis (i.e. average standard deviation of split frequencies <0.01, potential scale reduction factor (PRSF) close to 1.0, and effective sample size (ESS) > 200 in Tracer; Rambaut et al., 2018). All consensus trees were visualized and drawn using Figtree v. 1.4.4 (Rambaut, 2009) and modified with Adobe Illustrator CC2019.

Biogeographical analyses

We investigated the biogeography of the family Synlestidae using the parsimony ancestral state reconstruction function implemented in Mesquite (Maddison & Maddison, 2023). We created a new character matrix containing the geographic repartition of species according to five different subregions: Australia, Americas and Caribbean, Asia, Central Africa, Southern Africa (Supplemental material 3). We then coded the distribution of species according to the data available in Global Biodiversity Information Facility (GBIF) (https://www.gbif.org). Ultimately, we ran these analyses on our consensus Bayesian trees, without constraining the dispersal ability of taxa.

Specimen origins, imaging and examination

The Paskapoo Formation (Red Deer, Alberta) is a Paleocene unit from the western side of the Western Canada Sedimentary Basin (Glass, 1997). This formation was deposited in a fluvio-lacustrine environment by rivers flowing in an easterly direction (Hoffman & Stockey, 2000). The Paskapoo Formation is renowned for its abundant and well-preserved palaeofauna and palaeoflora, and it is mostly composed of interbedded hard to soft mudstone and sandstone, with subordinate pebble-conglomerate (Glass, 1997; Hoffman & Stockey, 2000). This formation was deposited by low-energy fluvial systems under humid conditions, with associated overbank environments including ponds and oxbow lakes (Hoffman & Stockey, 2000). The Paskapoo Formation is widespread in western Alberta, outcropping from the south in Calgary to the Hinton area (Hinton is a city north west to Calgary and west to Edmonton).

The Tiffanian Joffre locality, near Red Deer (Hoffman & Stockey, 2000, fig. 1), and the Blackfalds Insect and Plant Site, near Blackfalds, have yielded extremely well-preserved fossil material such as plants, mammals, fishes and insects (Baker & Wighton, 1984; Fox, 1990; Kevan & Wighton, 1981; LaPolla & Barden, 2018; Wighton, 1980, 1982; Wighton & Wilson, 1986; Wilson, 1996a, 1996b). The strata were dated by biostratigraphy to the middle Paleocene (Tiffanian) age using faunal remains (Fox, 1990, 1991), palynological data (Demchuk & Hills, 1991) and magnetostratigraphy (Lerbekmo et al., 1992). It is currently accepted that the age of the localities is *c.* 58–60 Ma (Ti$_3$ zone: Fox, 1990; 26r reverse polarity zone: Lerbekmo et al., 1992; P4 palynostratigraphic zonation: Demchuk, 1987, 1990).

The material described herein is currently housed in the Fossil Insect Collection (E. H. Strickland Entomological Museum) at the University of Alberta (Edmonton, UAPC or UAFIC). The specimens were studied using an Olympus SZX16stereomicroscope. Photographs were taken with a Nikon D90 with an attached 60 mm lens or with a Tagarno

Digital Microscope. All the photos were treated with graphic software. The figures were composed with Adobe Illustrator CC2019 and Photoshop CC2019 software.

Wing venation abbreviations

The nomenclature used for odonatan wing venation in this paper is based on the interpretations of Riek and Kukalová-Peck (1984), as modified by Nel et al. (1993) and Bechly (1996). The higher classification of fossil and extant Odonatoptera, as well as family and generic characters followed in the present work, is based on the phylogenetic system proposed by Bechly (1996) and Dijkstra et al. (2014) for the phylogeny of extant Zygoptera. Wing abbreviations are summarized in Nel and Piney (2022, fig. 20.1): **AA/AP**, anal vein (anterior/posterior); **Ax0/Ax1/Ax2**, primary antenodal cross veins; **arc**, arculus; **C**, costal vein; **Cr**, nodal cross vein; **CuA/CuP**, cubital vein (anterior/posterior); **CuAa** and **CuAb**, first distal posterior branches of CuA; **IR1** and **IR2**, supplementary convex longitudinal veins in radial area, emerging from the stem of RP; **MA/MP**, median vein (anterior/posterior); **MAa**, anterior branch of MA; **MAb**, posterior branch of MA, forming the distal side of the discoidal cell; **Mspl,** supplementary median vein between MA(a) and MP; **N** nodus; **o**, oblique crossvein between RP2 and IR2; **Pt**, pterostigma; **RA/RP**, radial vein (anterior/posterior) (RP is divided into three main branches RP1, RP2, and RP3/4); **Rspl,** supplementary radial vein between RP2 and IR2; **ScP**, posterior subcostal vein; **Sn**, subnodus.

Results

Phylogeny and biogeography

Our analyses result in two different topologies (Fig. 2). The support values for the extra-group relationships are good, except for a variation for the clade *Perilestes* + *Perissolestes*. The clade *Archilestes* + *Austrolestes* is well supported with posterior probabilities (PP) equal to 100 (Fig. 2A). Similarly, the monophyly of *Austrolestes* is well supported (PP = 96 or 98). The support for the clade *Perilestes* + *Perissolestes* depends on the analysis (PP equals 71 and 49, respectively) but is corroborated by the geographic distribution of these genera (Fig. 2).

The topology found under the rjMCMC analysis indicates that the genera *Ecchlorolestes* + *Nubiolestes* + *Chlorolestes* form a monophyletic clade (PP = 49), with a unique African origin (Fig. 2B). This clade is not found in the other analyses as *Ecchlorolestes* is grouped with the Australian genus *Synlestes* (PP = 43). Similarly, the position of the genus *Megalestes* greatly differs in our two analyses (Fig. 2). In the first, it is found close to the

clade *Episynlestes* + *Chorismagrion* + *Phylolestes* (PP = 76) while in the second it is found close to the genus *Synlestes* (PP = 50). The ancestral state reconstruction is better resolved in the rjMCMC analysis, with a unique origin of the African Synlestidae (Fig. 2B).

Systematic palaeontology

Order **Odonata** Fabricius, 1793
Suborder **Anisoptera** Selys-Longchamps and Hagen, 1854
Family **Gomphaeschnidae** Tillyard and Fraser, 1940
Subfamily **Gomphaeschninae** Tillyard and Fraser, 1940
Genus *Alloaeschna* Wighton and Wilson, 1986

Type species. *Alloaeschna paskapooensis* Wighton and Wilson, 1986.

Alloaeschna paskapooensis Wighton and Wilson, 1986

(Figs 3–7)

1986 *Alloaeschna marklae* Wighton and Wilson: 511, figs 9, 10 (syn. nov.)
1986 *Alloaeschna quadrata* Wighton and Wilson: 513, figs 11, 12 (syn. nov.)

Holotype. UAPC 6189 (= UAFIC 6189) (Fig. 3), part and counterpart collected by Betty A. Speirs on 3 November 1982, adult ♀ with right forewing and left hindwing joined to the thorax, four abdominal segments, and fragments of right leg(s); housed in the E. H. Strickland Entomological Museum at the University of Alberta (Edmonton, Canada).

Horizon and type locality. Paskapoo Formation, Paleocene (Tiffanian), Blackfalds Insect and Plant Site (Dennis Wighton's site 1), downstream from confluence with Blindman River, on left bank of Red Deer River, near Blackfalds, Alberta, Canada.

Additional material. *Alloaeschna marklae* Wighton and Wilson, 1986 syn. nov. (Fig. 4) UAPC 5553 (= UAFIC 5553), part and partial counterpart collected by Patricia Mitchell and Dennis C. Wighton in 1977, adult ♀ hindwing; housed in the E. H. Strickland Entomological Museum at the University of Alberta (Edmonton, Canada). Paskapoo Formation, Paleocene (Tiffanian), Blackfalds Insect and Plant Site (Dennis Wighton's site 1), downstream from confluence with Blindman River, on left bank of Red Deer River, near Blackfalds, Alberta, Canada.

Alloaeschna quadrata Wighton and Wilson, 1986 syn. nov. (Fig. 5), UAPC 6181/6268 (= UAFIC 6181/6268), part and counterpart collected by Betty A.
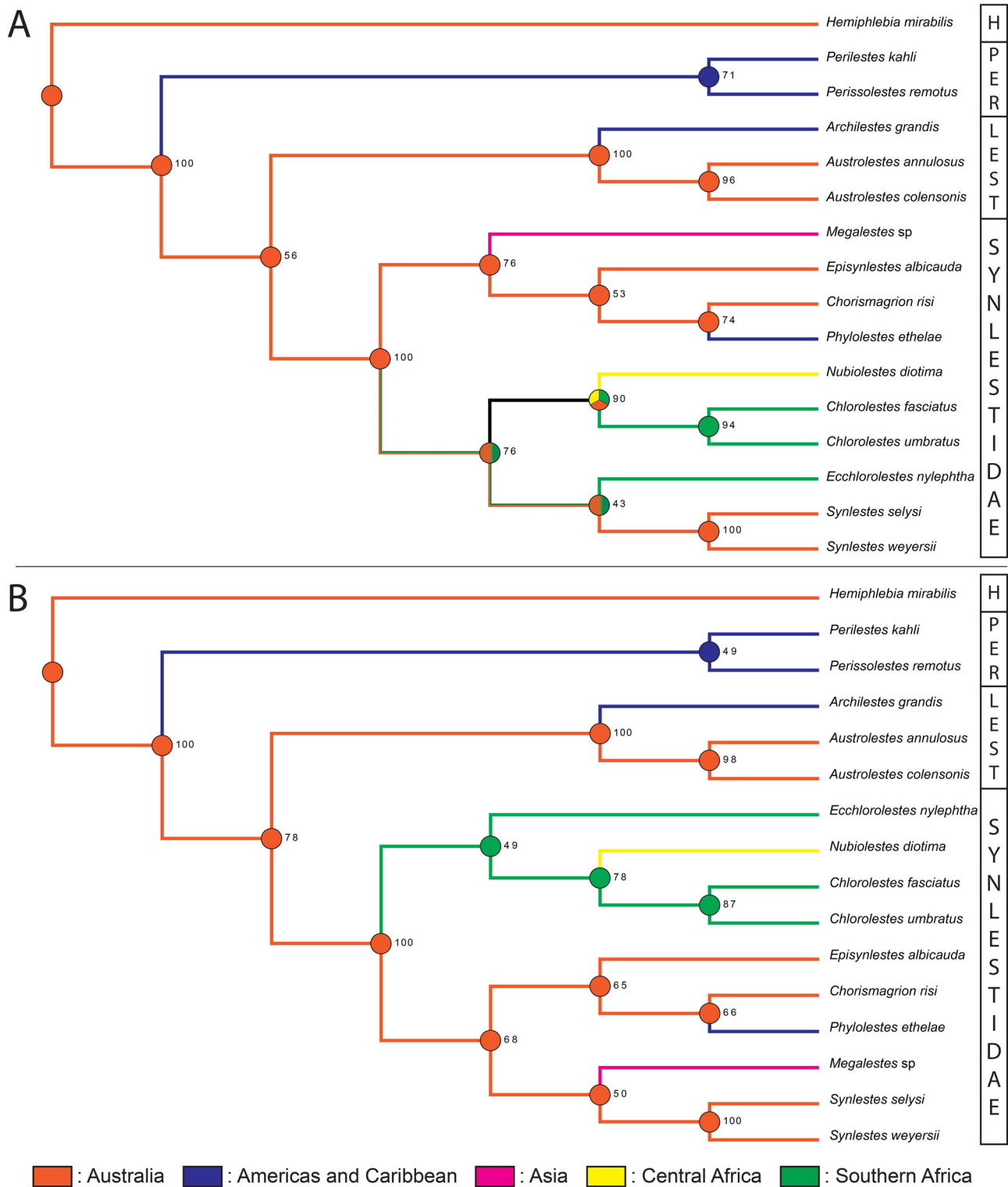
Figure 2. Bayesian trees resulting from our two analyses, with results of the parsimony ancestral state reconstruction for the biogeography indicated at the node and along branches. Values at nodes represent the posterior probabilities. **A**, using the models specified by PartitionFinder; **B**, using the reversible jump Markov chain Monte Carlo (rjMCMC) model. **Abbreviations**: **H**, Hemiphlebiidae; **Les**, Lestidae; **Per**, Perilestidae.
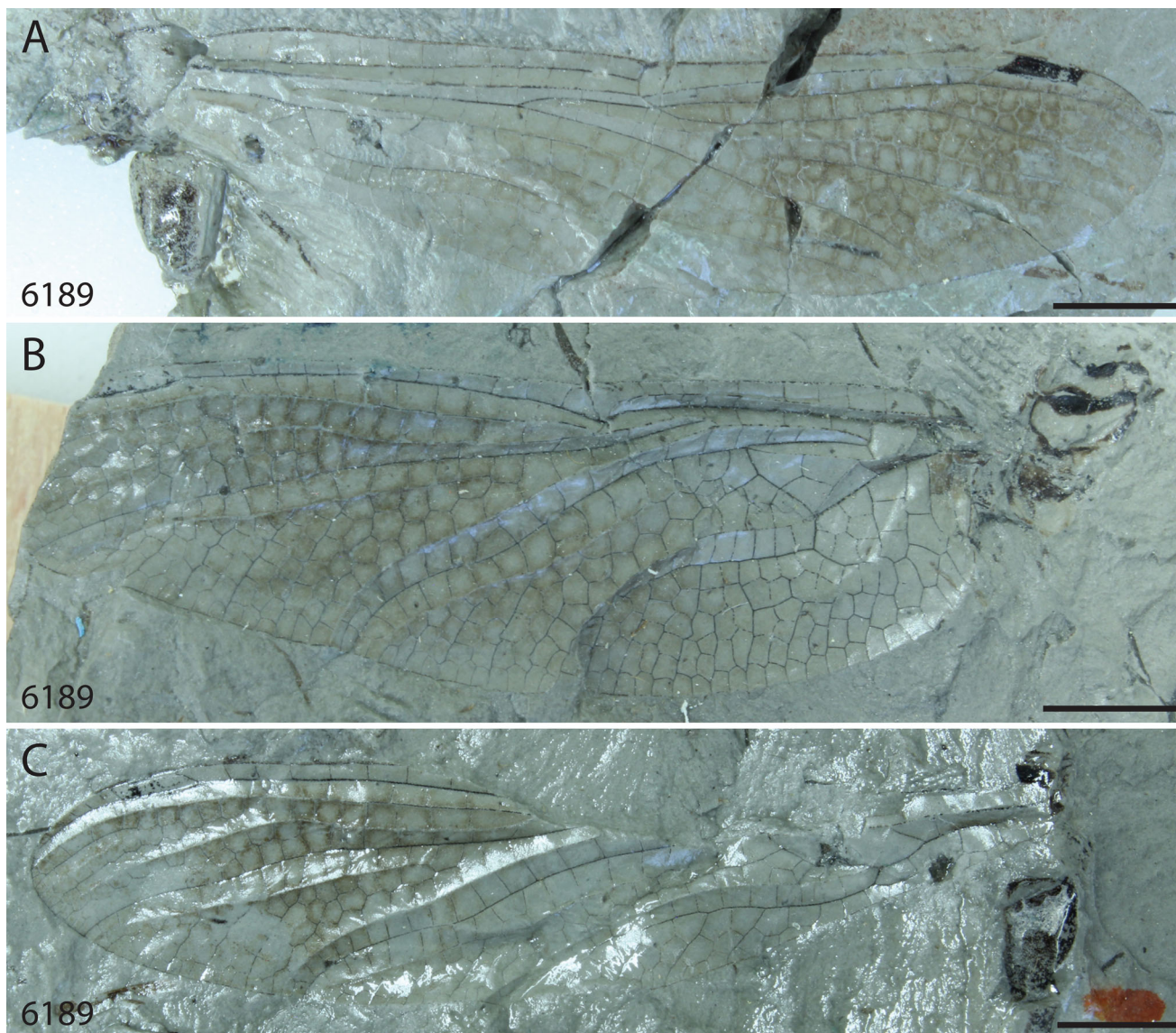
Figure 3. *Alloaeschna paskapooensis* Wighton and Wilson, 1986, holotype UAPC 6189 (= UAFIC 6189), Tiffanian of the Paskapoo Formation, Alberta, Canada. **A**, forewing; **B**, hind wing; **C**, forewing. Scale bars: 5 mm.

Speirs on 9 June 1980, adult forewing; housed in the E. H. Strickland Entomological Museum at the University of Alberta (Edmonton, Canada). Paskapoo Formation, Paleocene (Tiffanian), Joffre Bridge SW Insect layer (horizon C), Insect & Plant Layer, road cut on south side of Highway 11, west of 'missing infos', near Red Deer, Alberta, Canada.

New material. UAPC 6272/6266 (= UAFIC 6272/6266) part and counterpart collected by Betty A. Speirs in 1987 (Fig. 6), Joffre bridge SW Chert Layer, horizon B, road cut on south side of Highway 11; UAPC 6261/6265 (= UAFIC 6261/6265) part and counterpart collected by Betty A. Speirs in 1987 (Fig. 7), same locality as holotype.

Remarks. We provide a new photograph of the part illustrated in Wighton and Wilson (1986, figs 1, 2), and photographs of the counterpart not illustrated in Wighton and Wilson (1986, figs 3, 4). Similarly, we illustrate the part and counterpart of the specimen UAPC 6268/6185 (= UAFIC 6268/6185), while only UAPC 6185 was illustrated in Wighton and Wilson (1986).

Description. UAPC 6272/6266 (Fig. 6): a nearly complete forewing, without colouration pattern in preserved part; pterostigma dark brown; wing 10.6 mm wide; distance between arculus and nodus 15.3 mm; distance from nodus to pterostigma 15.0 mm; Ax2 well preserved; 13 antenodal crossveins of first row, 12 antenodal crossveins of second row; arculus angular;

Figure 4. *Alloaeschna marklae* Wighton and Wilson, 1986 syn. nov. UAPC 5553 (= UAFIC 5553), Tiffanian of the Paskapoo Formation, Alberta, Canada, hind wing. Scale bar: 5 mm.
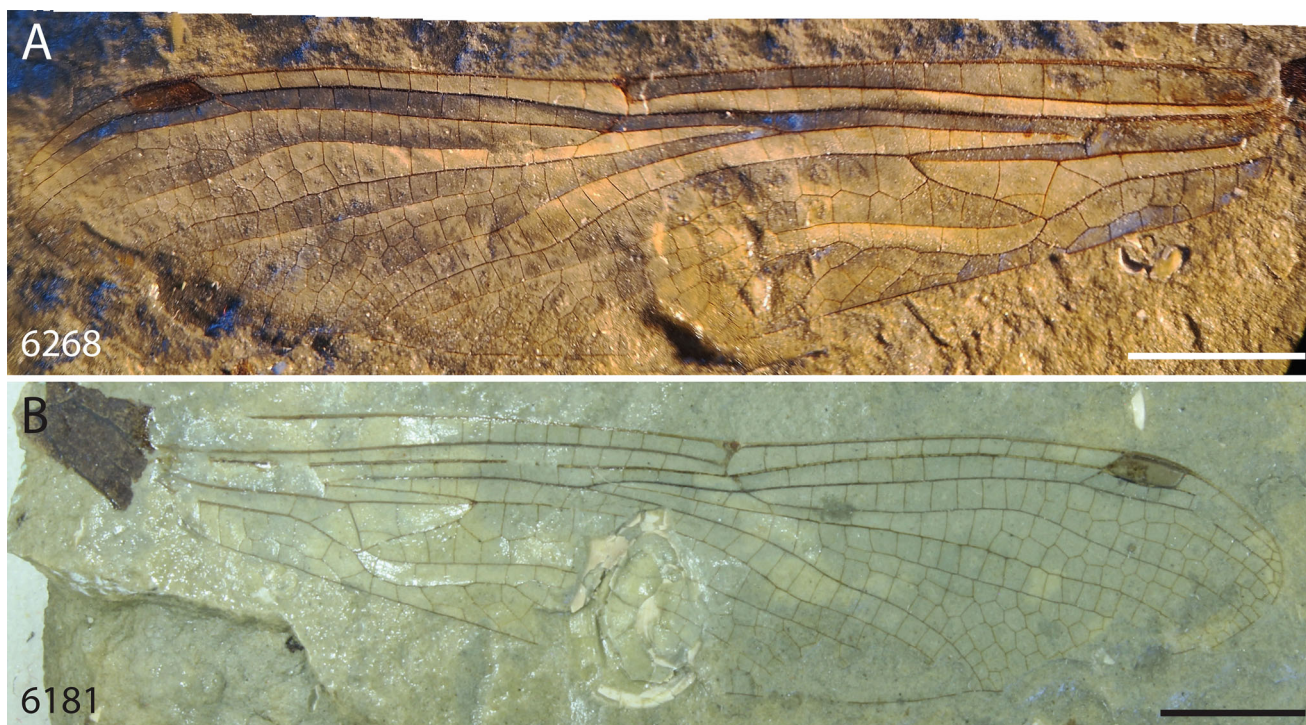

Figure 5. *Alloaeschna quadrata* Wighton and Wilson, 1986 syn. nov. UAPC 6181/6268 (= UAFIC 6181/6268), Tiffanian of the Paskapoo Formation, Alberta, Canada. **A**, part of forewing. **B**, counterpart of forewing. Scale bars: 5 mm.

pterostigma elongate and narrow, *c.* 1.05 mm wide, covering at least three cells, not basally recessed; pterostigmal brace strong, well aligned with basal side of pterostigma, strongly oblique; 10 postnodal crossveins not aligned with 10 postsubnodal crossveins; median space free; submedian space only traversed by CuP-crossing; hypertriangle free; discoidal triangle elongate, three-celled; MAb nearly straight, 4.8 mm long; a well-defined free subdiscoidal triangle; base of IR2 4.12 mm basal of nodus; base of RP3/4 5.3 mm basal of nodus; two crossveins between RP and IR2 basal of first oblique vein 'O'; first oblique vein 'O' 0.65 mm distad subnodus; area between RP1 and RP2 rather narrow with 2–3 rows of cells at level of pterostigma; base of RP2 well aligned with subnodus, RP2 smoothly undulated in its mid part; IR2 only slightly undulated, area
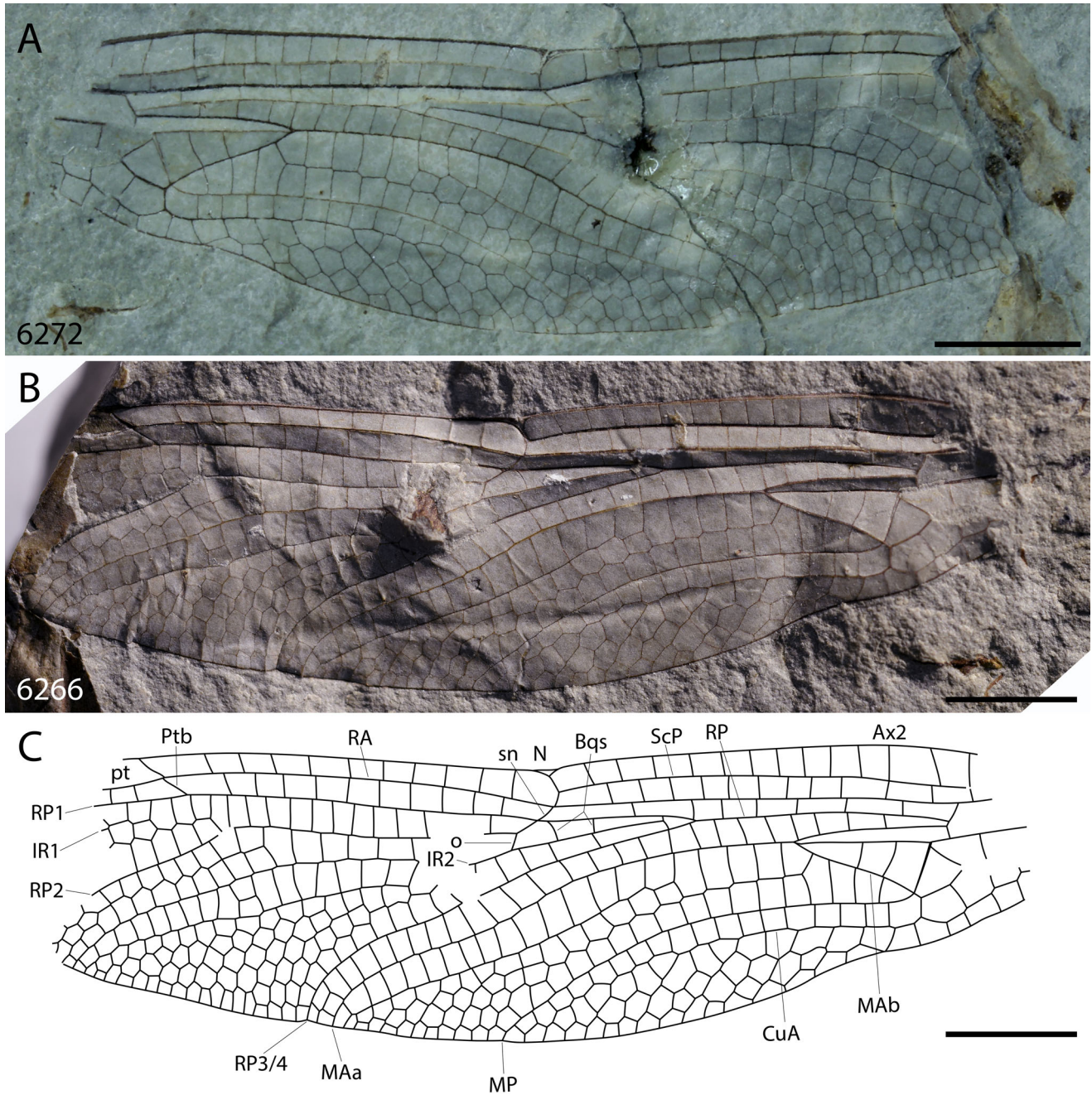
Figure 6. *Alloaeschna paskapooensis* Wighton and Wilson, 1986, additional specimen UAPC 6272/6266 (= UAFIC 6272/6266), Tiffanian of the Paskapoo Formation, Alberta, Canada. **A**, part of forewing; **B**, counterpart of forewing; **C**, interpretative drawing of forewing venation with main veins and structures labeled. **Abbreviations: Ax2,** primary antenodal crossvein; **Bqs,** bridge crossveins; **CuA,** anterior cubital vein; **IR1/IR2,** supplementary convex longitudinal veins in radial area, emerging from the stem of RP; **MP,** posterior median vein; **MAa,** anterior branch of MA; **MAb,** posterior branch of MA, forming the distal side of the discoidal cell; **N,** nodus; **o,** oblique crossvein between RP2 and IR2; **pt,** pterostigma; **Ptb,** pterositgmal brace; **RA/RP,** radial vein (anterior/posterior) (RP is divided into three main branches RP1, RP2, and RP3/4); **ScP,** posterior subcostal vein; **sn,** subnodus. Scale bars: 5mm.

between it and RP2 slightly widened in their undulated parts, with 2–3 rows of cells in its broadest part; IR2 and RP2 basally parallel, with only one row of cells; a well-developed and slightly undulated Rspl with 1–2 rows of cells between it and IR2; RP3/4 and MAa parallel and smoothly undulated, with one row of cells between them, except close to wing margin with two rows of cells; MAa and MP more or less parallel, post-discoidal area weakly widened with three rows of cells at level of nodus; no Mspl; MP and CuA basally
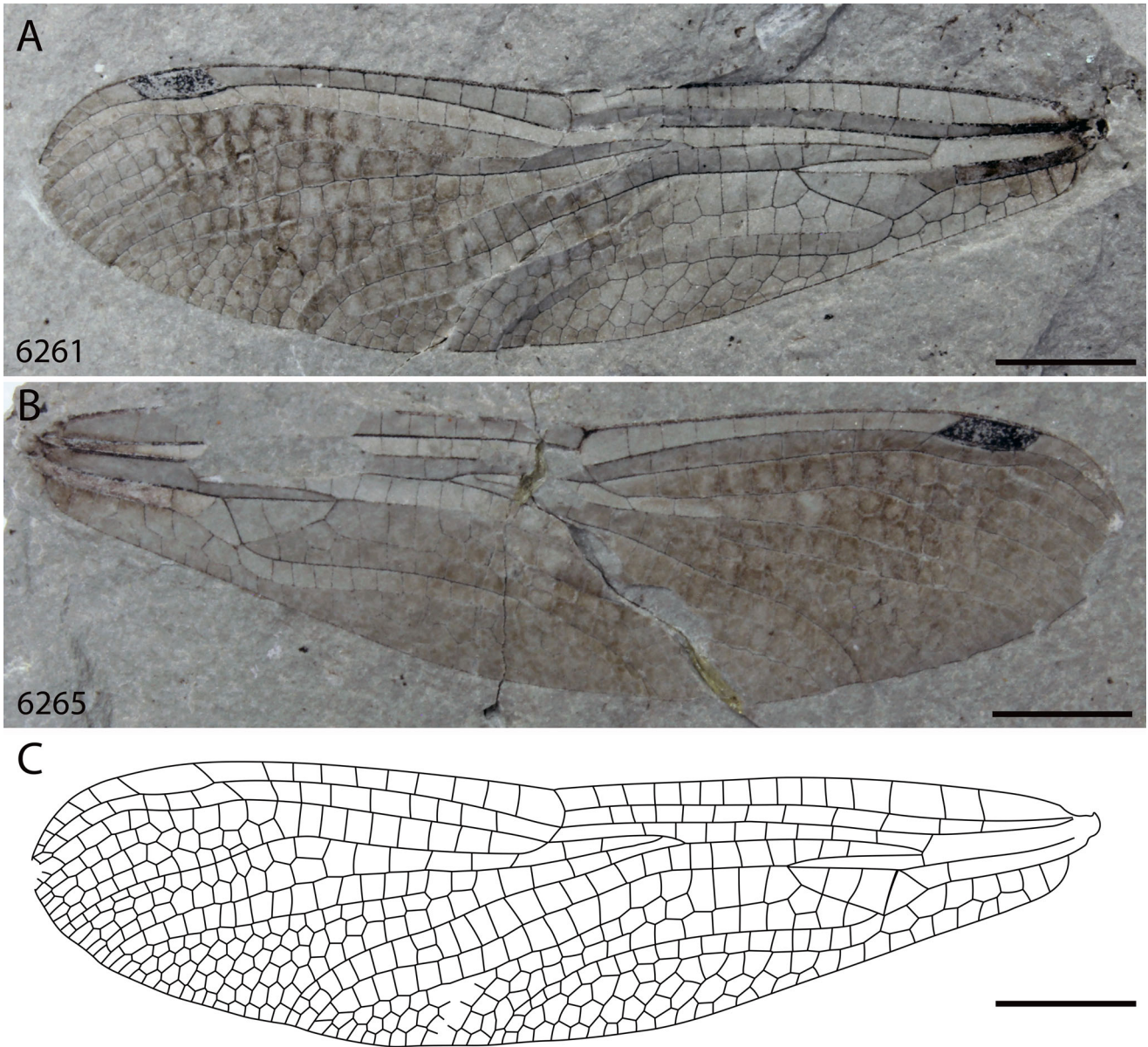
Figure 7. *Alloaeschna paskapooensis* Wighton and Wilson, 1986, additional specimen UAPC 6261/6265 (= UAFIC 6261/6265), Tiffanian of the Paskapoo Formation, Alberta, Canada. **A**, part of forewing; **B**, counterpart of forewing; **C**, interpretative drawing of wing venation. Scale bars: 5 mm.

parallel with one row of rectangular cells between them; CuA with six posterior branches, cubito-anal area with 4–5 rows of cells between CuA and posterior wing margin; two rows of cells in anal area.

UAPC 6261/6265 (Fig. 7): a complete forewing, with basal part of membrane infuscated; pterostigma dark brown; wing length 38.11 mm, 9.55 mm wide; distance between base and arculus 5.93 mm, between arculus and nodus 13.16 mm; distance from nodus to pterostigma 12.23 mm, from pterostigma to wing apex 5.08 mm; Ax1 and Ax2 well-preserved, with one antenodal crossvein between them; distance between Ax1 and wing

base 4.07 mm; 14 antenodal crossveins of first row, 11 antenodal crossveins of second row; arculus angular; pterostigma elongate and narrow, 2.66 mm long and 1.10 mm wide, covering three cells, not basally recessed; pterostigmal brace strong, well aligned with basal side of pterostigma, moderately oblique; nine postnodal crossveins not aligned with eight postsubnodal crossveins; median space free; submedian space only traversed by CuP-crossing; hypertriangle free; discoidal triangle elongate, three-celled; MAb slightly angled in its basal third, 3.93 mm long; a well-defined free subdiscoidal triangle; base of IR2 *c.* 3.55 mm basal of nodus;

base of RP3/4 *c.* 4.45 mm basal of nodus; two cross-veins between RP and IR2 basal of first oblique vein 'O'; first oblique vein 'O' *c.* 1 mm distad subnodus; pseudo-IR1 short, originating from RP1 below distal side of pterostigma; area between RP1 and RP2 rather narrow with 3–4 rows of cells between them; base of RP2 well aligned with subnodus, RP2 smoothly undulated in its mid-part; IR2 only slightly undulated, area between it and RP2 slightly widened at their undulated parts, with two rows of cell at level of undulation, three rows of cells between them distally; IR2 and RP2 basally parallel, with only one row of cells; RP3/4 and MAa parallel and smoothly undulated, with one row of cells between them, except just after undulation and distally with two rows of cells; MAa and MP more or less parallel, postdiscoidal area weakly widened with three rows of cells at level of nodus; no Mspl; MP and CuA basally parallel with one row of rectangular cells between them; CuA with six posterior branches, cubito-anal area with four rows of cells between CuA and posterior wing margin; two rows of cells in anal area.

Alloaeschna(?) nymph
(Fig. 8)

Material. UAPC 8502 (= UAFIC 8502) part collected by Betty A. Speirs in 1985; UAPC 8508 (= UAFIC 8508), part collected by Betty A. Speirs in 1983; housed in the E. H. Strickland Entomological Museum at the University of Alberta (Edmonton, Canada).

Horizon and locality. Paskapoo Formation, Paleocene (Tiffanian), Burbank, outcrops at the confluence of Red Deer River and Blindman River, about 1.2 km from the Blindman River localities, Alberta, Canada.

Description. UAPC 8502: A nearly complete nymph (with apex of the abdomen missing), possibly an exuvia because the head seems to be dorsally opened. Body brown without colouration pattern except on abdomen (see below), length *c.* 29.0 mm; head *c.* 5 mm long; mask partly preserved below head, apparently flat, of aeshnid type; eyes large, reniform. Thorax *c.* 6.0 mm long, with right hind leg preserved, femur *c.* 8.25 mm long; left wing pads putatively preserved. Abdomen quite long, at least 16.6 mm long, 8.1 mm wide, with a distinct colouration pattern: dorsally with a median uncoloured stripe bordered by another wider, brown line (on each side), these brown lines laterally bordered by an uncoloured stripe followed by another brown line (apparently separated from another brown line by an uncoloured stripe); seven segments preserved, of similar length but widening from base to apex, seventh the widest.

UAPC 8508: Body brown without colouration pattern except on abdomen (see below), length *c.* 29.5 mm. Head and thorax poorly preserved. Abdomen elongate, with a distinct colouration pattern: with a median uncoloured stripe bordered by another wider, brown line (on each side).

Remarks. We interpret these two specimens as *Alloaeschna* nymphs because they have proportions similar to those of the adults found in the same formation, apparently flat masks and the elongated abdomens typical of Aeshnoptera, and because of their patterns of colouration on the abdomen, similar to those of the extant *Gomphaeschna* spp. (Kennedy, 1936); also, to date, *Alloaeschna* is the sole anisopteran genus found in the Paskapoo Formation (despite abundant material having been collected for more than 30 years).

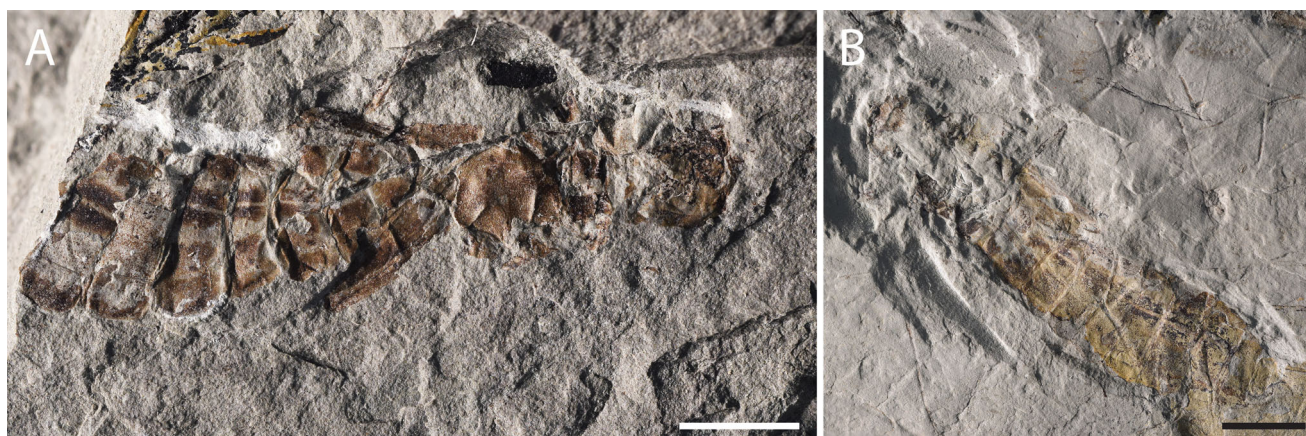### Genus and species indeterminate 1
(Fig. 9)

Figure 8. Putative nymphs of the genus *Alloaeschna*, Tiffanian of the Paskapoo Formation, Alberta, Canada. **A**, UAPC 8502 (= UAFIC 8502); **B**, UAPC 8508 (= UAFIC 8508). Scale bars: 5 mm.
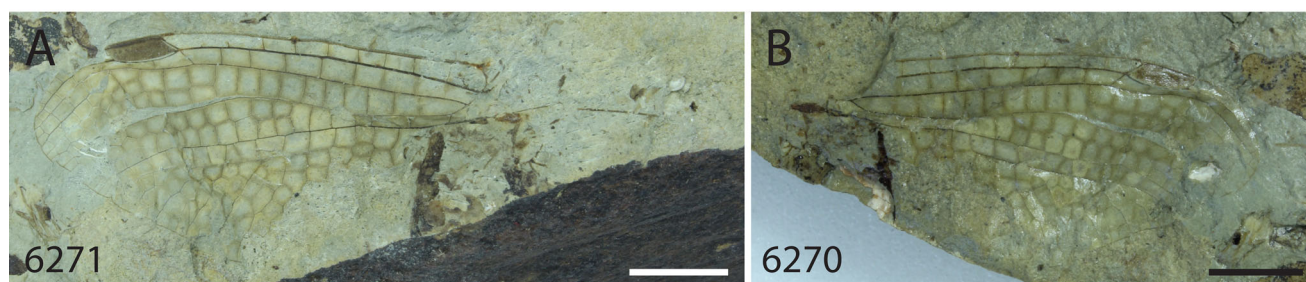
Figure 9. Indeterminate specimen of Gomphaeschnidae, UAPC 6170/6171 (= UAFIC 6170/6171), Tiffanian of the Paskapoo Formation, Alberta, Canada. Scale bars: 5 mm.

Material. UAPC 6170/6171 (= UAFIC 6170/6171) part and counterpart collected by Betty A. Speirs in 1984, adult forewing; housed in the E. H. Strickland Entomological Museum at the University of Alberta (Edmonton, Canada).

Horizon and locality. Paskapoo Formation, Paleocene (Tiffanian), Joffre Bridge SW Insect layer (horizon C), Insect & Plant Layer, road cut on south side of Highway 11, west of 'missing infos', near Red Deer, Alberta, Canada.

Description. Distal half of a wing, preserved part *c.* 31.5 mm long and *c.* 11.8 mm wide; nine postnodals not aligned with eight postsubnodals; pterostigma dark brown, short, *c.* 2.8 mm long and *c.* 1.3 mm wide (two and one-half cells long); pterostigmal brace not stronger than postsubnodals but distinctly oblique, well aligned with basal part of pterostigma; RP1 slightly undulating under and distad pterostigma; IR1 originating slightly distad pterostigma midlength; RP2 base aligned with subnodus, smoothly undulated in its mid-part, separated from RP1 by one row of cells until pterostigmal brace, then separated by at least two and at most four rows of cells; first oblique vein 'O' deformed, close to subnodus; IR2 only slightly undulated, basally parallel to RP2 (with only one row of cells between them), area between it and RP2 slightly widened at their undulated parts, with two rows of cell at level of undulation, at least three rows of cells between them distally; a distinct Rspl, straight and with one row of cells between it and IR2.

Remarks. The absence of a 'libelluloid' gap in the post-subnodal area, the pterostigmal brace aligned with basal side of pterostigma, the rather short pterostigma, and, overall, the area between RP1 and RP2 with only one row of cells up to one cell basad pterostigma level support an attribution to the Aeshnoptera rather than to the Petalurida, Gomphida or the 'libelluloid' clade. The presence of a well-defined Rspl but with only one row of cells between it and IR2 supports attribution to the Gomphaeschnidae. In fact, this wing is strongly similar

to those of *Alloaeschna* spp., but it is not possible to attribute it to a precise species or even genus.

Suborder **Zygoptera** Selys-Longchamps, 1854
Family **Synlestidae** Tillyard, 1917
Genus ***Albertalestes*** Jouault and Nel gen. nov.

Type species. *Albertalestes paskapooensis* sp. nov.

Etymology. The genus name is a combination of the name for the Canadian province of Alberta and the genus name *Lestes*. Gender neutral.

Diagnosis. Forewing with long main longitudinal veins; subdiscoidal cell posteriorly closed; elongate pterostigma (i.e. covering five and one-half cells); pterostigmal brace aligned with base of pterostigma; 'lestine' oblique cross-vein strong, three and a half cells distad RP fork (into RP1 and RP2); RP fork in first third of distance between nodus and pterostigma; base of RP3/4 basad subnodus, closer to nodus than to arculus; base of IR2 below nodus and slightly anteriad subnodus; area between MAa and RP3/4 wide along posterior margin of wing.

Albertalestes paskapooensis Jouault and Nel sp. nov.
(Figs 10, 11)

Type material. Holotype UAPC 6185 (= UAFIC 6185) (part and counterpart of a nearly complete wing) collected by David Maddison on 19 September 1981 (Fig. 10); paratype UAPC 6269 (= UAFIC 6269) (part of the distal two-thirds of a wing), collected by Betty A. Speirs in 1980 (Fig. 11A, B). All the type specimens are housed in the E. H. Strickland Entomological Museum at the University of Alberta (Edmonton, Canada).

Additional material. UAPC 8152 (= UAFIC 8152) (part and counterpart of the distal two-thirds of a wing), collected by Betty A. Speirs in 1993 (Fig. 11C–F); housed in the E. H. Strickland Entomological Museum at the University of Alberta (Edmonton, Canada).
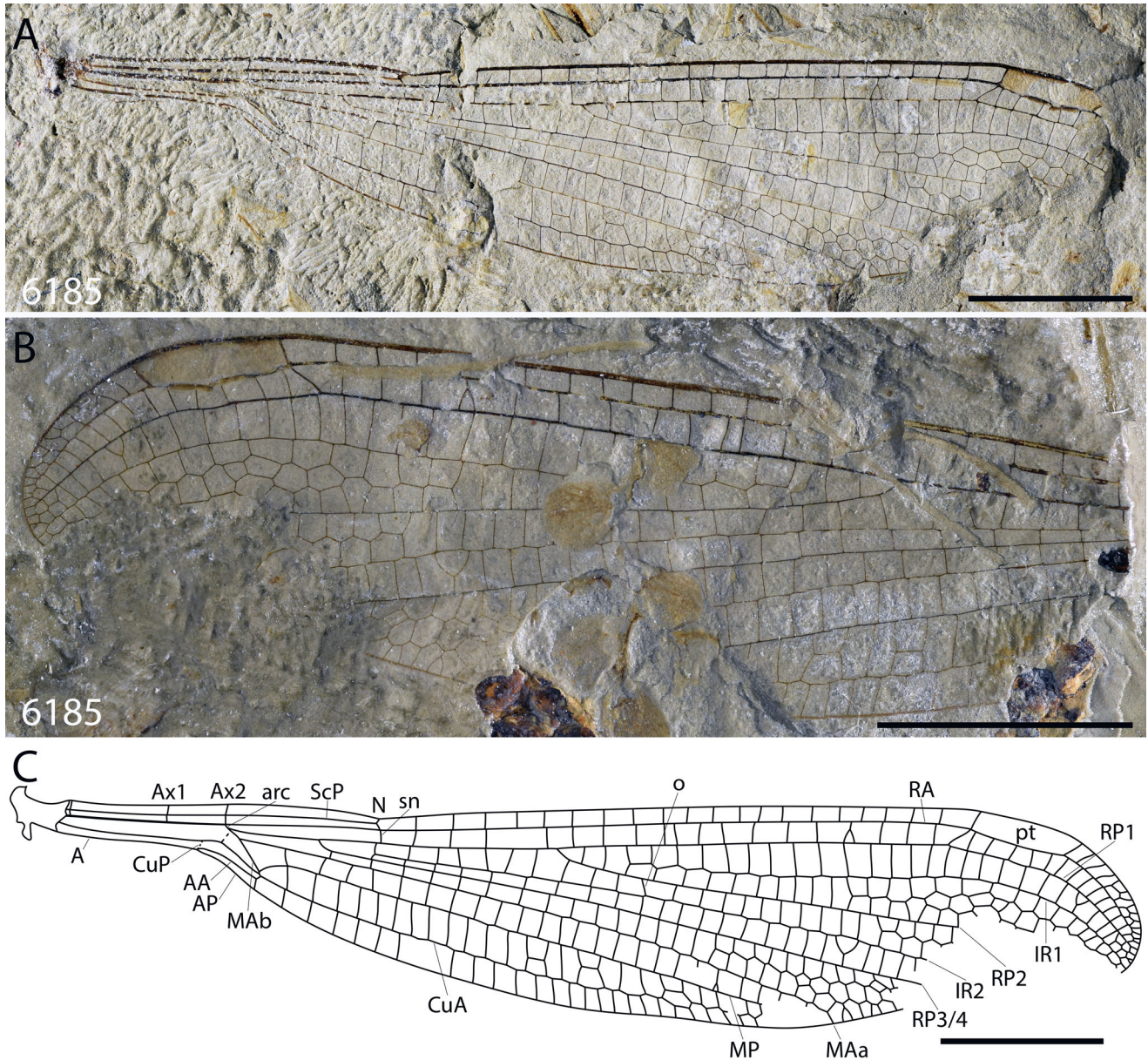
Figure 10. *Albertalestes paskapooensis* gen. et sp. nov., holotype UAPC 6185 (= UAFIC 6185), Tiffanian of the Paskapoo Formation, Alberta, Canada. **A**, part of forewing; **B**, counterpart of forewing; **C**, interpretative drawing of forewing venation with main veins and structures labelled. **Abbreviations: A,** anal vein; **AA/AP,** anal veins (anterior/ posterior); **Ax1/Ax2,** primary antenodal crossveins; **arc,** arculus; **CuA/CuP,** cubital vein (anterior/posterior); **IR1/IR2,** supplementary convex longitudinal veins in radial area, emerging from the stem of RP; **MP,** posterior median vein; **MAa,** anterior branch of MA; **MAb,** posterior branch of MA, forming the distal side of the discoidal cell; **N,** nodus; **o,** oblique crossvein between RP2 and IR2; **pt,** pterostigma; **RA/RP,** radial vein (anterior/posterior) (RP is divided into three main branches RP1, RP2, and RP3/4); **ScP,** posterior subcostal vein; **sn,** subnodus. Scale bars: 5mm.

Etymology. Named after the origin of the type material, i.e. the Paskapoo Formation.

Horizon and locality. Holotype (UAPC 6185): Paskapoo Formation, Paleocene (Tiffanian), Joffre Bridge (Site 5), near Red Deer, Alberta, Canada. Paratype (UAPC 6269): Paskapoo Formation, Paleocene (Tiffanian), Joffre Bridge SW Insect layer (horizon C), Insect & Plant Layer, road cut on south side of Highway 11, west of 'missing infos', near Red Deer, Alberta, Canada. Additional specimen (UAPC 8152): Paskapoo Formation, Paleocene (Tiffanian), Joffre Bridge SW Insect layer.

Diagnosis. As for the genus, by monotypy (see above).

Descriptions. The three wings are very similar (see Discussion, below). Holotype UAPC 6185 (Fig. 10):
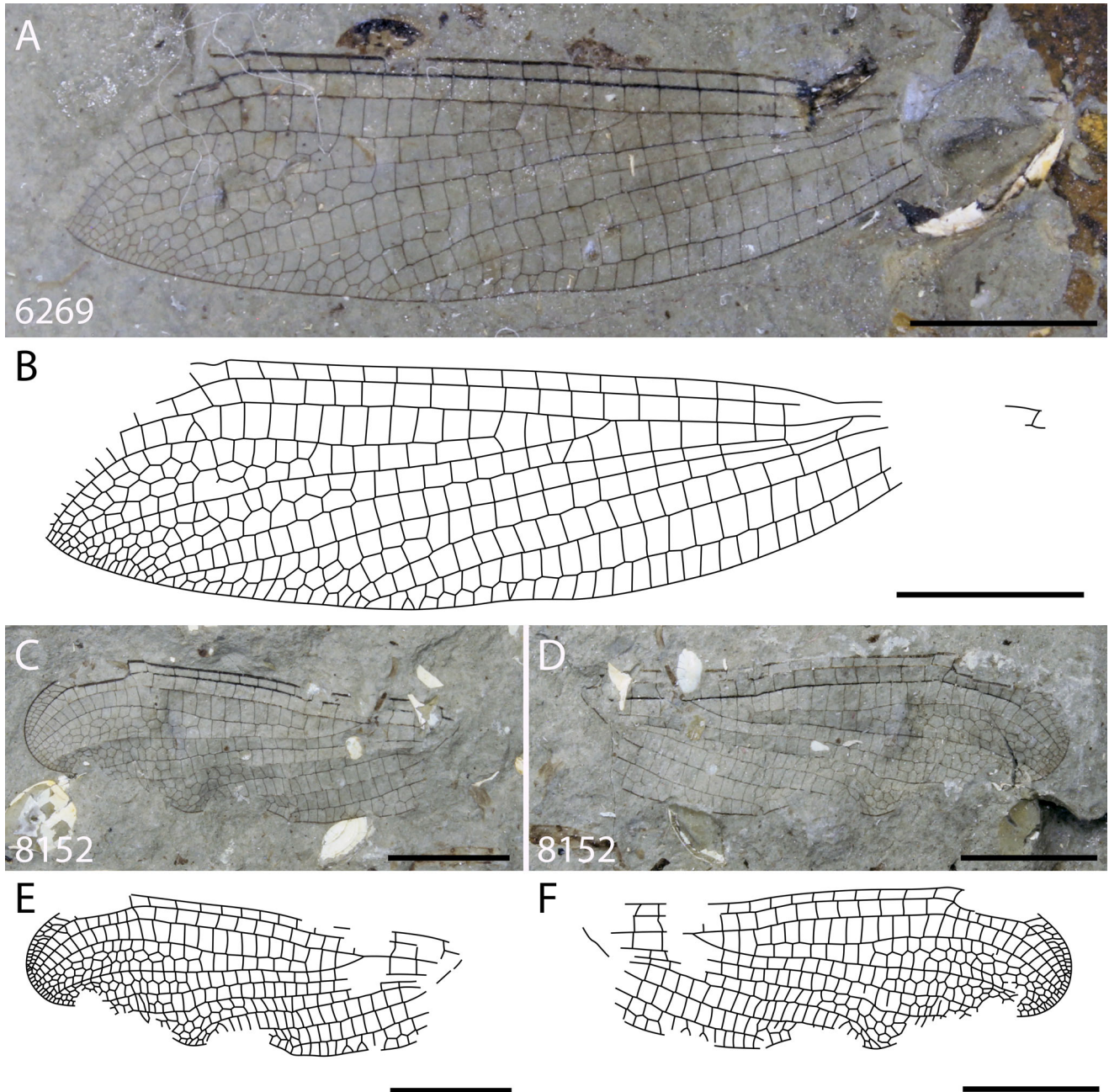
Figure 11. *Albertalestes paskapooensis* gen. et sp. nov., Tiffanian of the Paskapoo Formation, Alberta, Canada. **A**, paratype UAPC 6269 (= UAFIC 6269); **B**, interpretative drawing of paratype wing venation; **C**, part of referred specimen UAPC 8152 (= UAFIC 8152); **D**, counterpart of referred specimen UAPC 8152 (= UAFIC 8152); **E**, interpretative drawing of wing venation of part of UAPC 8152 (= UAFIC 8152); **F**, interpretative drawing of wing venation of counterpart of UAPC 8152 (= UAFIC 8152). Scale bars: 5 mm.

wing 32.7 mm long, 6.7 mm wide; petiole 5.5 mm long; distance from base to arculus 5.8 mm, from arculus to nodus 4.8 mm, from nodus to pterostigma 18.23 mm; from base to Ax1 4.02 mm, between Ax1 and Ax2 1.79 mm; arculus opposite Ax2; no secondary antenodal crossvein; antesubnodal space free; basal part of area between RP and MAa up to base of RP3/4 free; terminal kink of costal margin reduced at nodus; nodal furrow reduced; nodal crossing Cr moderately oblique; subnodus perpendicular to RP and RA; base of RP very close to base of arculus; stem of MA distinctly curved; MAa straight; stem of MA shorter than MAb; MAb 1.16 mm long, making an acute angle with MP + CuA; MP distinctly curved at its base (close to distal angle of discoidal cell), and distally straight; CuA nearly straight, with 1–2 rows of cells between it and MP; one row of

cells in cubital area; discoidal cell basally closed (crossvein between MA and MP + CuA incompletely preserved); subdiscoidal cell narrow elongate, posteriorly closed; base of AA and CuP midway between Ax1 and Ax2; base of RP3/4 situated at two-thirds of the distance between arculus and nodus, closer to nodus; base of IR2 situated below nodus, slightly anteriad subnodus; 20 postnodal crossveins, many of them not aligned with corresponding postsubnodals; pterostigma elongate, 3.12 mm long, 0.85 mm wide, covering five and one-half cells; pterostigmal brace not stronger than postsubnodals but distinctly oblique; space between C and RA distad pterostigma with *c.* 11 crossveins, two rows of cells in distal part; base of IR1 10.2 mm basad pterostigma (15 cells) and 2.2 mm distad base of RP2 (three cells); IR1 elongate, basally zigzagged and distally curved, with one row of cells between it and RP1, except close to wing margin with two rows of cells; base of RP2 five and a half cells distad subnodus, RP2 straight up to wing margin with a supplementary zigzagged longitudinal vein between it and IR1; a supplementary zigzagged longitudinal vein between RP2 and IR2; an oblique crossvein 'O' between RP2 and IR2 three and one-half cells distad base of RP2; IR2 and RP3/4 weakly curved, tapering slightly and gradually towards the wing margin, with one row of cells in between; one row of cells in postdiscoidal area up to wing margin.

Paratype UAPC 6269 (Fig. 11A, B): preserved part 26.9 mm long, wing 6.5 mm wide; distance from nodus to pterostigma 15.96 mm; 16 postnodal crossveins, many of them not aligned with corresponding postsubnodals; pterostigma elongate, covering at least four cells; oblique crossvein situated one cell distad base of RP2; base of RP2 four and a half cells distad subnodus.

Additional specimen UAPC 8152 (Fig. 11C–F): preserved part 17.9 mm long, wing 6.02 mm wide; distance from nodus to pterostigma 12.97 mm; at least 12 postnodal crossveins, many of them not aligned with corresponding postsubnodals; pterostigma elongate, 2.3 mm long, 0.75 mm wide, covering *c.* six and one-half cells.

Remarks. These three wings likely belong to the same taxon. We support this assertion as follows: (1) they differ only in the position of the 'lestine' oblique crossvein; (2) the base of RP2 is four cells distad in UAPC 6185 vs two in UAPC 6269; (3) the presence of 20 postnodal crossveins in UAPC 6185 vs 16 in UAPC 6269; and (4) base of RP2 five and one-half cells distad subnodus in UAPC 6185 versus four and one-half cells in UAPC 6269. These differences could be due to differences between the fore- and hind wings of the same taxon, or they could simply represent intraspecific variability.

Following the analysis of Bechly (2016), affinities with the Caloptera Belyshev and Haritonov, 1983 are excluded because of the presence of a distinctly oblique pterostigmal brace (less oblique in paratype and additional specimen due to deformation). By contrast, it has the putative synapomorphies of the Euzygoptera Bechly, 1996 (Lestomorpha Bechly, 1996, and Coenagrionomorpha Bechly, 1996). These include: (1) longitudinal veins rather straight and long; (2) only one row of cells between CuA and the hind margin of wings; (3) only the two primary antenodal brackets Ax1 and Ax2 are retained in the antenodal space; (4) antesubnodal space without any crossveins; and (5) no antefurcal crossveins present in the space between RP and MA from arculus to midfork. Affinities with the Coenagrionomorpha are excluded because the pterostigma is not shortened, the postnodal and postsubnodal crossveins are not well aligned, and the 'lestine' oblique vein is present (Bechly, 2016).

The Lestomorpha have no clear wing venation synapomorphies. Within this clade, affinities with the Hemiphlebiidae Tillyard, 1926 are excluded because the new fossils have a great number of postnodals, an oblique crossvein, RP1 not kinked at the insertion of the pterostigmal brace vein, and the presence of several secondary longitudinal veins. The new fossils share with the Cretaceous family Cretacoenagrionidae Bechly, 1996 (monotypic: *Cretacoenagrion alleni* Jarzembowski, 1990) the base of RP3/4 being closer to subnodus than to arculus, and the base of IR2 below the nodus and close to the subnodus (Jarzembowski, 1990). To date, there is no apomorphy to support the Cretacoenagrionidae, but the new fossils can be separated from this clade owing to their discoidal cell basally closed (vs open in *Cretacoenagrion alleni*), the highest number of postnodals (more than 12 vs nine), and the more developed venation between RP1 and RP2 (Jarzembowski, 1990, fig. 1).

The new fossils differ from the enigmatic Cretaceous genus *Cretalestes* Jarzembowski et al., 1998, in part because of the presence of the 'lestine' oblique crossvein (vs absent in *Cretalestes*), bases of RP3/4 and IR2 closer to nodus than to arculus (vs closer to arculus than to nodus), and the more developed venation between RP1 and RP2 (with at least four rows of cells vs two rows) (Jarzembowski et al., 1998, fig. 8).

The presence of an MP distinctly curved after its origin (at the distal angle of the discoidal cell) is a putative synapomorphy with Eulestiformia Bechly, 1996 (Chorismagrionidae Tillyard & Fraser, 1938 + Lestida Bechly, 1996). The Chorismagrionidae only includes the extant genus *Chorismagrion* Morton, 1914. The new fossils strongly differ from this genus because of their elongate pterostigma (vs short in *Chorismagrion*), the

presence of 'lestine' oblique crossvein, the base of IR2 close to subnodus (vs four cells more distal), and the base of RP3/4 basad subnodus (vs being below it) (Münz, 1919, fig. 69).

The Lestida (Perilestidae Tillyard & Fraser, 1938, Synlestidae Tillyard, 1917, Megalestidae Tillyard & Fraser, 1938, and Lestidae Calvert, 1901) have a basal closure of the discoidal cell, as in the new fossils (only visible in the holotype). The crossvein closing this cell is strongly oblique in the holotype as in the lestid genus *Archilestes* Selys, 1862 (Donnelly, 1981). The new fossils differ from the Perilestidae (*Perilestes* Hagen, 1862, *Perissolestes* Kennedy, 1941, *Palaeoperilestes* Zheng et al., 2016) because of their elongate pterostigma, the presence of the 'lestine' oblique crossvein (not preserved in the additional specimen but likely present), the base of IR2 below subnodus instead of being four cells more distal, base of RP3/4 basad subnodus instead of being distad it (Kennedy, 1941; Münz, 1919, fig. 70; Zheng et al., 2016). The Megalestidae and Lestidae generally share with the new fossils the presence of the 'lestine' oblique crossvein (absent in *Archilestes*) but differ from them because they have the bases of RP3/4 and IR2 closer to arculus than to nodus (Münz, 1919, figs 39–43). The Eocene family Eolestidae (*Eolestes* Cockerell, 1940) and the Paleocene family Menatlestidae Nel and Jouault, 2022 lack the 'lestine' oblique crossvein and have the bases of RP3/4 and IR2 closer to arculus than to nodus (Cockerell, 1940; Greenwalt & Bechly, 2014; Nel & Jouault, 2022). The Eocene genus *Lutetialestes* Greenwalt and Bechly, 2014 (uncertain family) has a different configuration of the bases of RP3/4 and IR2 (i.e. closer to arculus than to nodus: Greenwalt & Bechly, 2014).

The new fossil shows similarities to the Synlestidae in the positions of the bases of RP3/4 and IR2, the shape of the pterostigma, the presence of main longitudinal veins and their intercalaries, and the strongly oblique MAb. Collectively, we use these features to argue that the new fossils belong to this family. The new fossil differs from *Synlestes* Selys, 1868, *Episynlestes* Kennedy, 1920, *Nubiolestes* Fraser, 1945, and *Chlorolestes* Selys, 1862 in the subdiscoidal cell posteriorly closed vs opened, and the presence of the 'lestine' oblique crossvein (Kennedy, 1920; Münz, 1919, figs 63, 66; Schmidt, 1943). *Ecchlorolestes* Barnard, 1937 and the Eocene genera *Madres* Petrulevičius, 2018 and *Inacayalestes* Petrulevičius, 2015 have a 'lestine' oblique crossvein, but their subdiscoidal cell is often posteriorly opened (Barnard, 1937; Petrulevičius, 2015, 2018). The genus *Ecchlorolestes* also has a comparatively shorter pterostigma (i.e. covering fewer cells) (Ris, 1921). The genera *Phylolestes* Christiansen, 1948 and *Sinolestes* Needham, 1930 have a subdiscoidal cell posteriorly closed, often no

'lestine' oblique crossvein, and a narrower area between MAa and RP3/4 near posterior margin of wing (Christiansen, 1948; Needham, 1930; Schmidt, 1943). The new fossils also differ from *Sinolestes* because they have the base of IR2 below the nodus and subnodus (vs far distad nodus in *Sinolestes*) (Needham, 1930; To & Quang, 2018). Note that *Sinolestes* may have a crossvein interpreted as the 'lestine' oblique crossvein, but this crossvein is weak and always far distad the origin of RP2. The new fossils differ from the genus *Megalestes* Selys-Longchamps, 1862, at least, because of their elongate pterostigma, their IR2 originating below nodus and subnodus (vs well before in *Megalestes*) (Gyeltshen et al., 2017; Selys-Longchamps, 1862; Yu & Xue, 2020).

The Cretaceous genus *Gaurimacia* Vasilenko, 2005 shares with the new fossils a subdiscoidal cell posteriorly closed and a 'lestine' oblique crossvein, but differs from the latter in the much shorter main longitudinal veins (i.e. the entire wing is shorter in *Gaurimacia*), the base of RP2 in a distinctly more distal position (i.e. at mid-distance between nodus and pterostigma vs distinctly closer to nodus that to pterostigma in the new fossils), area between RP3/4 and IR2 not strongly narrowed near wing margin (vs widening close to wing margin), and the pterostigmal brace not aligned with base of pterostigma (Vasilenko, 2005, fig. 1). The Cretaceous genus *Cretaphylolestes* Huang et al., 2022 differs from the new fossil, at least because of the absence of the oblique vein and a distinctly shorter pterostigma (Huang et al., 2022). Therefore, we consider that the new fossils belong to a new genus and species that can be attributed to the Synlestidae. Recently, a new genus of the family Synlestidae has been described from the Paleocene of the Menat Formation as *Palaeophylolestes* Doriath-Döhler et al., 2023. The new specimen clearly differs from this genus, *inter alia*, because of its MAa, MP, and CuA that reach the posterior wing margin well before the pterostigma (vs reaching posterior wing margin very close or below the pterostigma in *Palaeophylolestes*: apomorphic to this genus).

The specimen UAPC 8152 is not placed in the type series because numerous characters in the basal part of the wing are not preserved. The configuration of the nodus and the configuration of the IR2 base, or the conformation of the discoidal and anal area, are unknown, while they are used in the diagnosis of the new genus.

Discussion

Phylogenetic reconstructions and their biogeographical implications

Our phylogenetic analyses in Bayesian inferences, when compared with the results of Simaika et al. (2020),

support similar relationships for a few genera but also conflict with the placement of some others (Fig. 2).

In our first analysis, we found the genera *Nubiolestes* and *Cholorestes* grouped together, forming the first African radiation of the Synlestidae (Fig. 2A). A group with the genera *Synlestes* and *Ecchlorolestes* would be a second African branch of the Synlestidae (Fig. 2A). In our second analysis, we found a monophyletic clade (*Ecchlorolestes* + *Nubiolestes* + *Chlorolestes*). This topology would indicate that the African Synlestidae have a single common origin (Fig. 2B). From a parsimony perspective, this second scenario is the more likely. To date, no fossil of the family Synlestidae is known from African deposits. Note that the posterior probabilities of these two conflicting topologies do not allow us to choose which is the best (Fig. 2). We suggest that including the genus *Sinolestes* may help to clarify this conflict, but no molecular data are available for this taxon.

Interestingly, the monophyletic clade (*Ecchlorolestes* + *Nubiolestes* + *Chlorolestes*), found in our second analysis, resembles the topology of Simaika et al. (2020), except that the genus *Phylolestes* is not nested within this clade (Fig. 2B). The position of *Megalestes* differs in all our analyses and from the results of previous analyses (Fig. 2; Simaika et al., 2020). In our data set, *Megalestes* is the only Asian species. We suggest that including *Sinolestes*, another Asian genus, in the analysis may help to clarify its position. The genus *Phylolestes* is found close to *Chorismagrion* in both analyses. This suggests that *Phylolestes* has independently dispersed into the Caribbean, having originated from the New World. This independent dispersion was also found in previous analyses (Simaika et al., 2020).

The biogeographical history of the family Synlestidae results from millions of years of speciation and extinction processes. The latter are difficult to disentangle

using the extant diversity of the clade (i.e. a reduced number of species), and the scarce fossil record of the family. Nevertheless, it is known that the Cretaceous and Paleocene species of Synlestidae were distributed in relatively cold and temperate biomes in the northern hemisphere (North America and Asia; Fig. 12). This indicates that the distribution of the family has greatly changed through time and has likely been shaped by numerous geological and environmental events (Himalayan uplift, PETM biome changes, glaciations). In fact, the pre-PETM distribution is hardly comparable with the current distribution of the family because no synlestids are known from North America or southern South America today (Fig. 12). Extant species of the family are found in central Asia, eastern Australia, and southern Africa, and in Central America and the Caribbean (Fig. 12).

There are several hypotheses to explain the decline of the family in North America. The most likely one is that the temperate biome extension towards high latitude, that occurred during the PETM, may have affected the habitats of *Albertalestes*, leading to its disappearance and to that of other putative synlestids inhabiting North America (Fig. 12). For instance, it has been suggested that changes in plant groups in terrestrial environments have often triggered faunal changes in past freshwater insect faunas (Sinitshenkova, 2003). The second hypothesis would be that other odonatan lineages outcompeted the Synlestidae, leading the latter to decline. This double-wedge pattern, in which one clade declines while the other thrives, is well documented in the fossil record (Sepkoski, 1996). A similar hypothesis has been proposed to explain the decline of the Palaeodictyoptera during the Permian Period, which were outcompeted by the Hemiptera (Labandeira, 1997).

Similarly, the extinction of the Synlestidae in the southern part of South America can be explained by
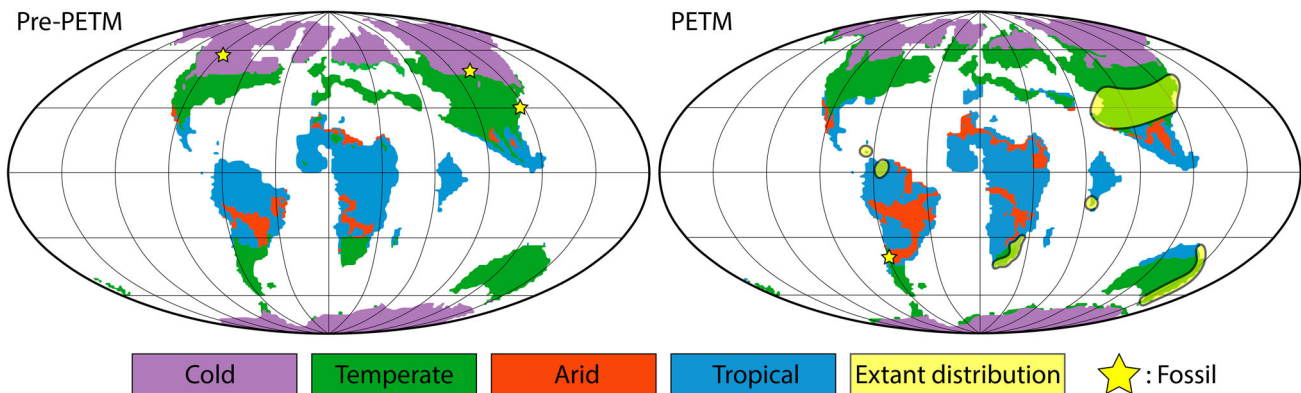

Figure 12. Changes in late Paleocene biomes with the distribution of fossil and extant Synlestidae indicated (modified from Korasidis et al., 2022).

'similar' hypotheses (Fig. 12). First, environmental modifications in the region (e.g. uplift of the Andes, aridification) are known to have greatly shaped the diversity dynamics of many plant, vertebrate and invertebrate lineages (e.g. Pérez-Escobar et al., 2022). It would not be surprising if they also affected the Synlestidae. During the Eocene, much of South America and Africa became arid (Herold et al., 2014). This aridification has constrained the distribution (migration) of some clades and caused others to decline due to local extinctions (Aria et al., 2023; Jouault et al., 2021). The extant Synlestidae are mainly found in areas where tropical or warm-temperate forests were present during the Eocene (northern South America, southern east of Africa, eastern part of Australia and central region of Asia). It would not be surprising if the Synlestidae had taken refuge in certain areas with biomes favourable to their survival (Fig. 12).

Therefore, we suggest that the Synlestidae experienced several extinction events throughout their evolutionary history. We believe that a holistic phylogenetic analysis encompassing all the fossil and extant diversity of the Zygoptera would provide further insight into the evolution of the clade and allow us to resolve unanswered questions such as their local extinction.

Refining the limits of the *Alloaeschna* species

The genus *Alloaeschna* was initially divided into three species (Wighton & Wilson, 1986) largely based on the configuration of the discoidal triangle (divided into two or three cells) and the conformation of the ribs (i.e. horizontal in *A. quadrata*, while vertical in the other species). However, plasticity of this part of the wing is extremely high in the family Aeshnidae (closely related to the Gomphaeschnidae), and the use of these characters in separating species has been suggested to be unreliable (Nel et al., 1994). The perfect illustration of this variability is found in the extant genus *Aeshna*, for which a specimen can have a different number of crossveins in the discoidal triangle or the submedian space between its left and right wings (see *Aeshna* cf. *juncea*: Fig. 13A). This variability, and the poor diagnostic value of this character, were pointed out over 100 years ago by Cockerell (1908). We further illustrate the plasticity of wing venation in Aeshnidae by providing an illustration of a specimen of *Heliaeschna fuliginosa* Karsch, 1893 in which there is a different conformation of the discoidal triangle between the left and right forewings and also between the left and right hind wings (Fig. 13B).

All the lengths of the *Alloaeschna* forewings presented in this study fall in the intraspecific range of variability known for extant species of Aeshnoidea (38–

45 mm) (Aguesse, 1968). They also have similar widths (c. 9–10 mm) and similar discoidal triangle length-to-width ratios (0.4–0.45). The new specimens of *A. paskapooensis* also fill the gap originally recorded for the number of antenodals between *A. quadrata* and *A. paskapooensis*, with a first row composed of 13 or 14 crossveins and a second row of 9–12 crossveins (Wighton & Wilson, 1986). Moreover, the new specimens indicate that the number of postnodals can vary between 9 and 11 and the number of postsubnodals from 7 to 10. Previously the species *A. quadrata* was thought to be different from *A. paskapooensis* because its pterostigma was covering more cells (3.3 vs 2.6), but the new specimen UAPC 6261/6265 has a pterostigma covering three cells, which fills the gap used to separate the two species (Wighton & Wilson, 1986).

Another argument used previously to justify the separation of *A. quadrata* from *A. paskapooensis* was the colouration patterns present at the base of the wings of *A. quadrata* and assumed to be absent in *A. paskapooensis* (Wighton & Wilson, 1986). If the wing colouration patterns are indeed useful to separate species (e.g. Jouault et al., 2022), it is important to consider the intraspecific variability of these patterns but also their possible 'maturation' between a young individual (teneral) and an older individual. Indeed, during the maturation period dragonflies often lack their adult colouration, a phenomenon well documented in many present-day genera (e.g. *Calopteryx*, *Crocothemis*). In the present specimens, we notice the presence of darkened areas at the base of the hind wing of *A. paskapooensis* (Fig. 3B), which completely limits the diagnostic value of this character to separate *Alloaeschna* species. Therefore, in our opinion, it is impossible to reliably separate *A. quadrata* from *A. paskapooensis*.

The type specimen of *A. marklae* is poorly preserved and deformed. The deformation questions the diagnostic value of the angle (i.e. outer margin of triangle sharply angled anteriorly) used to separate *A. marklae* from *A. paskapooensis* (Wighton & Wilson, 1986). Those authors also proposed that the presence of a discoidal triangle with two cells, and a supratriangle (= submedian space) with one crossvein, are diagnostic features, but as discussed above these characters are extremely plastic and cannot be used to separate species (Wighton & Wilson, 1986). All the differences between *A. marklae* and *A. paskapooensis* fall within the range of intraspecific variability. Based on these comparisons, we consider the species *A. quadrata* and *A. marklae* to be junior synonyms of *A. paskapooensis*, and consequently synonymized these two species under *A. paskapooensis*.
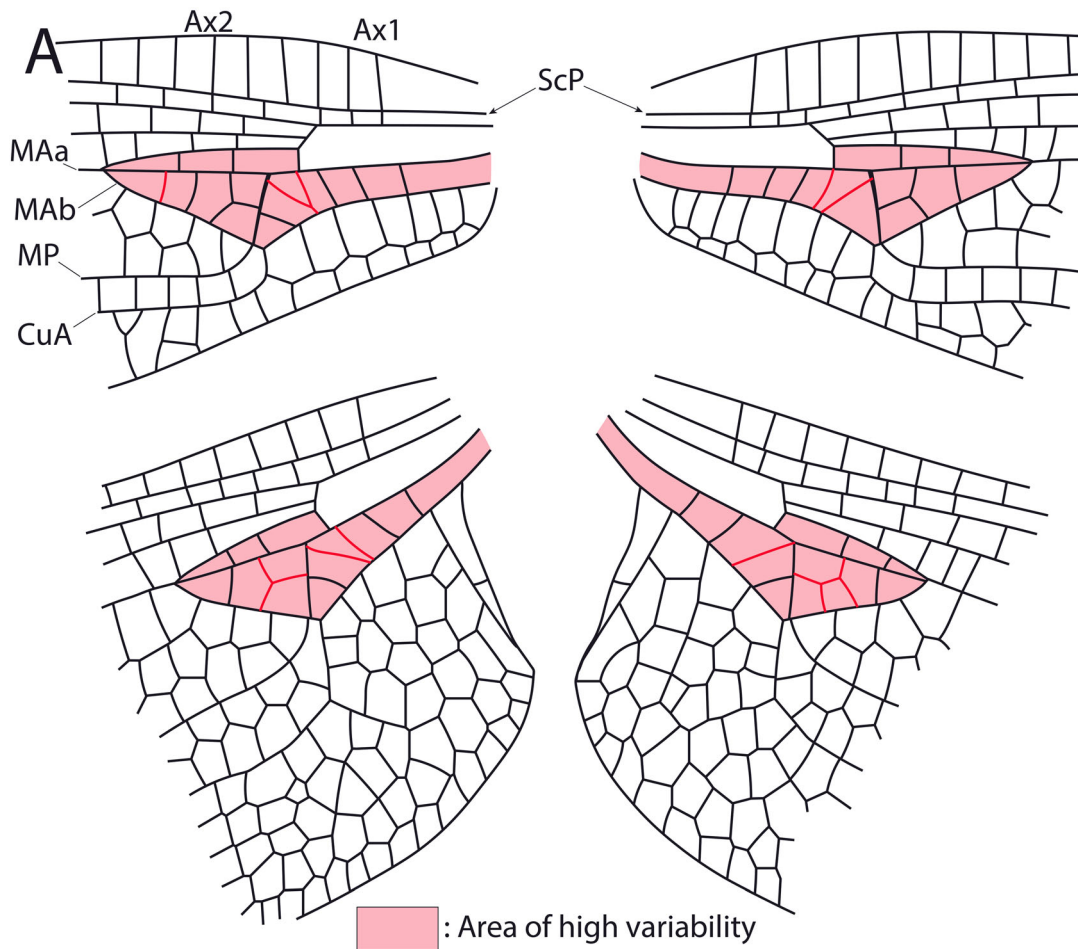
Figure 13. Illustration of variability and plasticity in Aeshnidae species. **A**, line drawing of wing bases of an extant specimen of *Aeshna* cf. *juncea* with main veins labelled; **B**, photograph of *Heliaeschna fuliginosa* Karsch, 1893, specimen housed in MNHN. **Abbreviations: Ax1/Ax2,** primary antenodal crossveins; **CuA,** cubital vein anterior; **MAa,** anterior branch of MA; **MAb,** posterior branch of MA, forming the distal side of the discoidal cell; **MP,** posterior median vein; **ScP,** posterior subcostal vein. Scale bar: 2mm.

Palaeoecological implications of the presence of nymphs or exuviae

Fossil nymphs or exuviae of Odonata are rather rare, and in most cases, adults are found without associated nymphs or exuviae (e.g. Nel & Jouault, 2022; Nel et al., 2022). This differential fossilization is partially explained by the development of hemimetabolous insects in which the larvae and the adults often live in different environments (i.e. aquatic larval stage). If this type of development provides advantages (e.g. occupation of distinct ecological niches), it biases the fossil record. In fact, the fossilization sites of adults can be distinct and far from the place where the nymphs lived and developed (i.e. rivers and lakes vs forests or more open habitats), with different chemical proprieties. Consequently, this complicates the assignment of a given nymph to a species described based solely on images. This issue may result in two scenarios; the description and placement of the nymphs in a distinct genus – which artificially increases the diversity of the clade – or the assignment of nymphs to the wrong genus.

In the present case, the two nymphs or exuviae are interpreted as belonging to the genus *Alloaeschna*, even if it is impossible to certify this as a fact (Fig. 8). The discoveries of nymphs or exuviae in the same formation (and relatively close to each other in terms of distance) lead us to hypothesize that the fossilization area encompasses the place where both the larvae developed and the adults lived. Following this hypothesis and considering the fluvial origin of the Paskapoo Formation – previously interpreted to be deposited principally in fluvial to floodplain environments (e.g. Hoffman & Stockey, 2000) – and the fossil record (Glass, 1997; Hoffman & Stockey, 2000), the Paskapoo Formation was dominated by a freshwater environment with aquatic vegetation and water of relatively good quality (allowing the development of the larvae). In fact, Hoffman and Stockey (2000) described diverse stratigraphic units interpreted as representing five freshwater depositional environments (flood plain, fluvial channel, abandoned channel, swamp, and crevasse splay). The sandstones exhibit cross-bedding structures, ranging from medium- to coarse-grained, characteristic of river channel deposits (Hoffman & Stockey, 2000). Significantly, the sandstones contain conglomeratic material. The siltstones and mudstones rich in plant fossils, as well as the presence of palaeosols, have been interpreted as indicating the presence of crevasse splays, overbank areas, and shallow swamps (see Hoffman & Stockey, 2000 for more detail). By comparison, the larvae of the extant species of *Gomphaeschna* (one of the closest extant relatives) live in *Sphagnum* bogs, 'cedar' swamp on aquatic herbaceous plants and/or in small pools (Dunkle, 1977; Kennedy, 1936). The larvae of Odonata are fierce predators feeding on other aquatic invertebrates or small vertebrates from their immediate environment, and we suggest that *Alloaeschna* nymphs were likely able to predate other large invertebrates because of their large size. In the Paskapoo Formation, numerous larvae of Tipulidae (and other unidentified Diptera), some Ephemeroptera, and aquatic Coleoptera have been documented providing a sufficient diversity of prey for Anisoptera larvae (Mitchell & Wighton, 1979; Wighton, 1980).

An alternative scenario would be that the dried exuviae, which are quite robust and enduring objects, have been transported by winds (allochthonous deposit). This phenomenon is thought to occur for exuviae trapped in amber (Bechly & Wichard, 2008). In fact, the exuviae and amber are quite unlikely to encounter each other naturally because amber is produced, most of the time, above the ground while larvae of Odonata develop in water. Therefore, it is assumed that the dried exuviae or nymphs found in amber were transported by winds that trapped them in resin flows, or that the larvae got stuck in resin flow when climbing on the trunks or grasses surrounding the water for their imaginal moult. Another unlikely scenario is that resin falls directly into the water on a nymph and engulfs it *in situ*. Nevertheless, if the 'allochthonous hypothesis' is retained, it is possible that the two specimens belong either to the genus *Alloaeschna* or to another undescribed anisopteran genus that lived in Alberta during the Paleocene.

Conclusions

Our phylogenetic analyses, based on molecular data, suggest that conflicting topologies can be found when reconstructing synlestid evolution. In our present state of knowledge, it is difficult to decide which biogeographical scenario occurred. The description of the first zygopteran from the Paskapoo Formation, namely *Albertalestes paskapooensis* gen. et sp. nov., increases the fossil diversity of the family Synlestidae. This new taxon and two early Eocene synlestid genera in Argentina indicate that this family was much more widespread in the past, and likely experienced several local extinction events. Several drivers may be responsible for these extinctions, but we suggest that biome modifications during the Palaeogene are likely involved. The study of new specimens of the genus *Alloaeschna* suggests that the previous diversity of the genus was artefactual and that only one species was present in the Paskapoo Formation. In fact, the new specimens fill

gaps in character variability used previously to separate the three constitutive species of the genus. This revision led to the synonymization of *A. marklae* syn. nov. and *A. quadrata* syn. nov. with *A. paskapooensis*.

Disclosure statement

No potential conflict of interest was reported by the author(s).

Supplemental material

Supplemental material for this article can be accessed here: http://dx.doi.org/10.1080/14772019.2023.2261457.

ORCID

Corentin Jouault http://orcid.org/0000-0002-3680-5172
Baptiste Coutret http://orcid.org/0000-0002-0893-0638
Kurt O. Konhauser http://orcid.org/0000-0001-7722-7068
André Nel http://orcid.org/0000-0002-4241-7651

References

Aguesse, P. (1968). Les Odonates de L'Europe occidentale, du nord de l'Afrique et des Îles Atlantiques. *Faune de l'Europe et du Bassin méditerranéen*, *4*, 1–258.

Aria, C., Jouault, C., Perrichot, V., & Nel, A. (2023). The megathermal ant genus *Gesomyrmex* (Formicidae: Formicinae), palaeoindicator of wide latitudinal biome homogeneity during the PETM. *Geological Magazine*, *160*, 187–197. https://doi.org/10.1017/S0016756822001248

Baker, G. T., & Wighton, D. C. (1984). Fossil aquatic oribatid mites (Acari, Oribatida, Hydrozetidae: *Hydrozetes*) from the Paleocene of South-Central Alberta, Canada. *The Canadian Entomologist*, *116*, 773–775. https://doi.org/10.4039/Ent116773-5

Barden, P., & Ware, J. L. (2017). Relevant relicts: The impact of fossil distributions on biogeographic reconstruction in ants and dragonflies. *Insect Systematics and Diversity*, *1*, 73–80. https://doi.org/10.1093/isd/ixx005

Barnard, K. H. (1937). Notes on dragonflies (Odonata) of the SW Cape with descriptions of the nymphs and of new species. *Annals of the South African Museum*, *32*, 169–260. https://biostor.org/reference/111670

Bechly, G. (1996). Morphologische Untersuchungen am Flügelgeader der rezenten Libellen und deren Stammgruppenvertreter (Insecta; Pterygota; Odonata), unter besonderer Berücksichtigung der Phylogenetischen Systematik und des Grundplanes der Odonata. *Petalura*, *2*, 1–402.

Bechly, G. (2016). Phylogenetic systematics of Odonata. https://bechly.lima-city.de/phylosys.htm

Bechly, G., Nel, A., Martínez-Declòs, X., Jarzembowski, E. A., Coram, R., Martill, D., Fleck, G., Escuillié, F., Wisshak, M. M., & Maisch, M. (2001). A revision and phylogenetic study of Mesozoic Aeshnoptera, with description of numerous new taxa (Insecta: Odonata: Anisoptera). *Neue Paläontologische Abhandlungen*, *4*, 1–219.

Bechly, G., & Wichard, W. (2008). Damselfly and dragonfly nymphs in Eocene Baltic amber (Insecta: Odonata), with aspects of their palaeobiology. *Palaeodiversity*, *1*, 37–73.

Christiansen, K. A. (1948). A new genus and species of damselfly from Southern Haiti (Odonata). *Psyche*, *54*, 256–262. https://doi.org/10.1155/1947/59418

Cockerell, T. D. A. (1908). Description of Tertiary insects. *American Journal Sciences*, *24*, 69–75. https://doi.org/10.2475/ajs.s4-25.147.227

Cockerell, T. D. A. (1940). A dragon-fly from the Eocene of Colorado (Odonata, Agrionidae). *Entomological New*, *51*, 103–105.

Coiro, M., Allio, R., Mazet, N., Seyfullah, L. J., & Condamine, F. L. (2023). Reconciling fossils with phylogenies reveals the origin and macroevolutionary processes explaining the global cycad biodiversity. *New Phytologist*. https://doi.org/10.1111/nph.19010

Condamine, F. L., Clapham, M. E., & Kergoat, G. (2016). Global patterns of insect diversification: Towards a reconciliation of fossil and molecular evidence?. *Scientific Reports*, *6*, 19208. https://doi.org/10.1038/srep19208

Condamine, F. L., Silvestro, D., Koppelhus, E. B. & Antonelli, A. (2020). The rise of angiosperms pushed conifers to decline during global cooling. *Proceedings of the National Academy of Sciences of the United States of America*, *117*, 28867–28875. https://doi.org/10.1073/pnas.200557111

Crisp, M. D., Trewick, S. A., & Cook, L. G. (2011). Hypothesis testing in biogeography. *Trends in Ecology & Evolution*, *26*, 66–72. https://doi.org/10.1016/j.tree.2010.11.005

Demchuk, T. D. (1987). *Palynostratigraphy of Paleocene strata of the central Alberta Plains* [Unpublished MSc

thesis]. University of Alberta. https://doi.org/10.7939/R3SX64K77

Demchuk, T. D. (1990). Palynostratigraphic zonation of Paleocene strata in the central and south-central Alberta Plains. *Canadian Journal of Earth Science*, 27, 1263–1269. https://doi.org/10.1139/e90-136

Demchuk, T. D., & Hills, L. V. (1991). A re-examination of the Paskapoo Formation in the central Alberta Plains: The designation of three new members. *Bulletin of Canadian Petroleum Geology*, 39, 270–282. https://doi.org/10.35767/gscpgbull.39.3.270

Dijkstra, K. D. B., Kalkman, V. J., Dow, R. A., Stokvis, F. R., & Van Tol, J. (2014). Redefining the damselfly families: A comprehensive molecular phylogeny of Zygoptera (Odonata). *Systematic Entomology*, 39, 68–96. https://doi.org/10.1111/syen.12035

Doriath-Döhler, A., Hervet, S., & Béthoux, O. (2023). *Palaeophylolestes distinctus* n. gen., n. sp., a new malachite damselfly (Odonata: Zygoptera: Synlestidae) from the Paleocene Menat locality (France). *Geodiversitas*, 45, 401–407. http://geodiversitas.com/45/14 https://doi.org/10.5252/geodiversitas2023v45a14

Dunkle, S. W. (1977). Larvae of the genus *Gomphaeschna* (Odonata: Aeshnidae). *The Florida Entomologist*, 60, 223–225. https://doi.org/10.2307/3493912

Fleck, G., Nel, A., & Martínez-Delclòs, X. (1999). The oldest record of libellulid dragonflies from the Upper Cretaceous of Kazakhstan (Insecta: Odonata, Anisoptera). *Cretaceous Research*, 20, 655–658. https://doi.org/10.1006/cres.1999.0166

Fox, R. C. (1990). The succession of Paleocene mammals in western Canada. in T. M. Bown & T. K. Rose (Eds.), *Dawn of the age of mammals in the northern part of the Rocky Mountain interior, North America*. Geological Society of America, 243, 51–70. https://doi.org/10.1130/SPE243-p51

Fox, R. C. (1991). Systematic position of *Pronothodectes gaoi* Fox from the Paleocene of Alberta: Reply. *Journal of Vertebrate Paleontology*, 64, 700–701. https://doi.org/10.1017/S0022336000030833

Glass, D. (1997). Lexicon of Canadian stratigraphy, *Western Canada including Eastern British Columbia*, Alberta, Saskatchewan and **southern Manitoba**. *Canadian Society of Petroleum Geologists*, 4, 772.

Greenwalt, D. E., & Bechly, G. (2014). A re-description of the fossil damselfly *Eolestes syntheticus* Cockerell, 1940 (Odonata: Zygoptera: Eolestidae n. fam.) with description of new taxa from the Eocene of North America. *Zootaxa*, 3887, 138–156. https://doi.org/10.11646/zootaxa.3887.2.2

Gyeltshen, T., Kalkman, V. J., & Orr, A. G. (2017). Honouring His Royal Highness the Crown Prince of Bhutan: *Megalestes gyalsey* (Odonata: Synlestidae). *Zootaxa*, 4244, 588–594. https://doi.org/10.11646/zootaxa.4244.4.9

Halsch, C. A., Shapiro, A. M., Fordyce, J. A., Nice, C. C., Thorne, J. H., Waetjen, D. P., & Forister, M. L. (2021). Insects and recent climate change. *Proceedings of the National Academy of Sciences of the United States of America*, 118, e200254311. https://doi.org/10.1073/pnas.2002543117

Herold, N., Buzan, J., Seton, M., Goldner, A., Green, J. A. M., Müller, R. D., Markwick, P., & Huber, M. (2014). A suite of early Eocene (∼55 Ma) climate model boundary conditions. *Geoscientific Model Development*, 7, 2077–2090. https://doi.org/10.5194/gmd-7-2077-2014

Hoffman, G. L., & Stockey, R. A. (2000). Geological setting and paleobotany of the Joffre Bridge Roadcut fossil locality (late Paleocene), Red Deer Valley, Alberta. *Canadian Journal of Earth Sciences*, 36, 2073–2084. https://doi.org/10.1139/e99-095

Huang, D., Fu, Y., Lian, X., Gao, J., & Nel, A. (2022). The oldest malachite damselfly (Odonata: Synlestidae) from the Lower Cretaceous of China. *Cretaceous Research*, 129, 105023. https://doi.org/10.1016/j.cretres.2021.105023

Huelsenbeck, J. P., Larget, B., & Alfaro, M. E. (2004). Bayesian phylogenetic model selection using reversible jump Markov chain Monte Carlo. *Molecular Biology and Evolution*, 21, 1123–1133. https://doi.org/10.1093/molbev/msh123

Huelsenbeck, J. P., & Ronquist, F. (2001). MRBAYES: Bayesian inference of phylogeny. *Bioinformatics*, 17, 754–755. https://doi.org/10.1093/bioinformatics/17.8.754

Jarzembowski, E. A. (1990). Early Cretaceous zygopteroids of southern England with the description of *Cretacoenagrion alleni*, gen. nov., spec. nov. (Zygoptera, Coenagrionidae, 'Anisozygoptera': Tarsophlebiidae, Euthemistidae). *Odonatologica*, 19, 27–37.

Jarzembowski, E. A., Martinez-Declos, X., Bechly, G., Nel, A., Coram, R., & Escullié, F. (1998). The Mesozoic non-calopterygoid Zygoptera: Description of new genera and species from the Lower Cretaceous of England and Brazil and their phylogenetic significance (Odonata, Zygoptera, Coenagrionoidea, Hemiphleboidea, Lestoidea). *Cretaceous Research*, 19, 403–444. https://doi.org/10.1006/cres.1997.0113

Jouault, C., Aase, A., & Nel, A. (2021). Past ecosystems drive the evolution of the early diverged Symphyta (Hymenoptera: Xyelidae) since the earliest Eocene. *Fossil Record*, 24, 379–393. https://doi.org/10.5194/fr-24-379-2021

Jouault, C., Ngo-Muller, V., Zhang, Q., & Nel, A. (2020). New empidoid flies (Diptera: Atelestidae; Dolichopodidae) from mid-Cretaceous Burmese amber. *Palaeoentomology*, 3, 204–211. https://doi.org/10.11646/palaeoentomology.3.2.10

Jouault, C., Tischlinger, H., Henrotay, M., & Nel, A. (2022). Wing coloration patterns in the Early Jurassic dragonflies as potential indicator of increasing predation pressure from insectivorous reptiles. *Palaeoentomology*, 5, 305–318. https://doi.org/10.11646/palaeoentomology.5.4.3

Katoh, K., & Standley, D. M. (2013). MAFFT Multiple Sequence Alignment Software Version 7: Improvements in performance and usability. *Molecular Biology and Evolution*, 30, 772–780. https://doi.org/10.1093/molbev/mst010

Kennedy, C. H. (1920). Forty-two hitherto unrecognized genera of Zygoptera. *Ohio Journal of Science*, 21, 83–88. https://doi.org/10.5962/bhl.part.14540

Kennedy, C. H. (1936). The habits and early stages of the dragonfly *Gomphaeschna furcillata* (Say). *Proceedings of the Indiana Academy of Science*, 45, 315–322.

Kennedy, C. H. (1941). Perilestinae in Ecuador and Peru: Revisional notes and descriptions (Lestidae: Odonata). *Annals of the Entomological Society of America*, 34, 658–688. https://doi.org/10.1093/aesa/34.3.658

Kevan, D. K. M. E., & Wighton, D. C. (1981). Paleocene orthopteroids from South-Central Alberta, Canada.

Canadian Journal of Earth Sciences, *18*, 1824–1837. https://doi.org/10.1139/e81-170

Kohli, M., Letsch, H., Greve, C., Béthoux, O., Deregnaucourt, I., Liu, S., Zhou, X., Donath, A., Mayer, C., Podsiadlowski, L., Gunkel, S., Machida, R., Niehuis, O., Rust, J., Wappler, T., Yu, X., Misof, B., & Ware, J. (2021). Evolutionary history and divergence times of Odonata (dragonflies and damselflies) revealed through transcriptomics. *IScience*, *24*, 103324. https://doi.org/10.1016/j.isci.2021.103324

Korasidis, V. A., Wing, S. L., Shields, C. A., & Kiehl, J. T. (2022). Global changes in terrestrial vegetation and continental climate during the Paleocene–Eocene Thermal Maximum. *Paleoceanography and Paleoclimatology*, *37*, e2021PA004325. https://doi.org/10.1029/2021PA004325

Labandeira, C. C. (1997). Insect mouthparts: Ascertaining the paleobiology of insect feeding strategies. *Annual Review of Ecology and Systematics*, *28*, 153–193. https://doi.org/10.1146/annurev.ecolsys.28.1.153

Lanfear, R., Frandsen, P. B., Wright, A. M., Senfeld, T., & Calcott, B. (2016). PartitionFinder 2: New methods for selecting partitioned models of evolution for molecular and morphological phylogenetic analyses. *Molecular Biology and Evolution*, *34*, 772–773. https://doi.org/10.1093/molbev/msw260

LaPolla, J. S., & Barden, P. (2018). A new aneuretine ant from the Paleocene Paskapoo Formation of Canada. *Acta Palaeontologica Polonica*, *63*, 435–440. https://doi.org/10.4202/app.00478.2018

Larsson, A. (2014). AliView: A fast and lightweight alignment viewer and editor for large data sets. *Bioinformatics*, *30*, 3276–3278. https://doi.org/10.1093/bioinformatics/btu531

Lerbekmo, J. F., Demchuk, T. D., Evans M. E., & Hoye, G. S. (1992). Magnetostratigraphy and biostratigraphy of the continental Paleocene of the Red Deer Valley, Alberta, Canada. *Bulletin of Canadian Petroleum Geology*, *40*, 24–35. https://doi.org/10.35767/gscpgbull.40.1.024

Maddison, W. P., & Maddison, D. R. (2023). Mesquite: A modular system for evolutionary analysis. Version 3.81. http://www.mesquiteproject.org

Mitchell, P., & Wighton, D. (1979). Larval and adult insects from the Paleocene of Alberta, Canada. *The Canadian Entomologist*, *111*, 777–782. https://doi.org/10.4039/Ent111777-7

Münz, P. A. (1919). A venational study of the suborder Zygoptera (Odonata) with keys for the identification of genera. *Memoirs of the Entomological Society*, *3*, 1–78. https://doi.org/10.5962/bhl.title.8499

Needham, J. G. (1930). A manual of the dragonflies of China. A monographic study of the Chinese Odonata. *Zoologia Sinica*, *11*, 1–344.

Nel, A. (2021). Maastrichtian representatives of the dragonfly family Aeschnidiidae question the entomofaunal turnover of the early Late Cretaceous. *Palaeoentomology*, *4*, 209–212. https://doi.org/10.11646/palaeoentomology.4.3.5

Nel, A., DePalma, R. A., & Engel, M. S. (2010). A possible hemiphlebiid damselfly in Late Cretaceous amber from South Dakota (Odonata: Zygoptera). *Transactions of the Kansas Academy of Science*, *113*, 231–234. https://doi.org/10.1660/062.113.0312

Nel, A., & Jouault, C. (2022). The odonatan insects from the Paleocene of Menat, central France. *Acta Palaeontologica Polonica*, *67*, 631–648. https://doi.org/10.4202/app.00960.2021

Nel, A., Martinez-Delclos, X., Escuillé, F., & Brisac, P. (1994). Les Aeshnidae fossiles: Etat actuel des connaissances. (Odonata, Anisoptera). *Neues Jahrbuch für Geologie und Paläontologie, Abhandlungen*, *194*, 143–186. https://doi.org/10.1127/njgpa/194/1994/143

Nel, A., Martínez-Delclòs, X., Paicheler, J.-C., & Henrotay, M. (1993). Les 'Anisozygoptera' fossiles. Phylogénie et classification (Odonata). *Martinia*, *3*, 1–311.

Nel., A., Nam, G. S., & Jouault, C. (2022). First representative of the odonatan superfamily Triassolestoidea (Odonatoptera: Parazygoptera) from the Upper Triassic of the Korean Peninsula. *Alcheringa: An Australasian Journal of Palaeontology*, *46*, 237–243. https://doi.org/10.1080/03115518.2022.2130426

Nel, A., & Piney, B. (2022). The Odonatoptera: A clade that contains 99% of Odonata fossil diversity. In A. Cordoba-Aguilar, C. Beatty, & J. Bried (Eds.), *Dragonflies and damselflies: Model organisms for ecological and evolutionary research* (2nd ed.) (pp. 279–294). Oxford Academic. https://doi.org/10.1093/oso/9780192898623.003.0020

Pérez-Escobar, O. A., Zizka, A., Bermúdez, M. A., Meseguer, A. S., Condamine, F. L., Hoorn, C., Hooghiemstra, H., Pu, Y., Bogarín, D., Boschman, L. M., Pennington, R. T., Antonelli, A., & Chomicki, G. (2022). The Andes through time: Evolution and distribution of Andean floras. *Trends in Plant Science*, *27*, 364–378. https://doi.org/10.1016/j.tplants.2021.09.010

Petrulevičius, J. F. (2015). A new Synlestidae damselfly (Insecta: Odonata: Zygoptera) from the early Eocene of Nahuel Huapi Este, Patagonia, Argentina. *Arquivos Entomolóxicos*, *14*, 287–294. http://sedici.unlp.edu.ar/handle/10915/99440

Petrulevičius, J. F. (2018). A new malachite damselfly (Synlestidae: Odonata) from the Eocene of Patagonia, Argentina. *Life: The Excitement of Biology*, *6*, 36–43. https://doi.org/10.9784/LEB6(2)Petrulevicius.01

Rambaut, A. (2009). FigTree v.1.4.4. http://tree.bio.ed.ac.uk/software/figtree/

Rambaut, A., Drummond, A. J., Xie, D., Baele, G., & Suchard, M. A. (2018). Posterior summarisation in Bayesian phylogenetics using Tracer 1.7. *Systematic Biology*, *67*, 901–904. https://doi.org/10.1093/sysbio/syy032

Riek, E. F., & Kukalová-Peck, J. (1984). A new interpretation of dragonfly wing venation based upon Early Carboniferous fossils from Argentina (Insecta: Odonatoidea) and basic characters states in pterygote wings. *Canadian Journal of Zoology*, *62*, 1150–1166. https://doi.org/10.1139/z84-166

Ris, F. (1921). The Odonata or dragonflies of South Africa. *Annals of the South African Museum*, *18*, 282–283. https://doi.org/10.5962/bhl.part.8026

Ronquist, F., & Huelsenbeck, J. P. (2003). MrBayes 3: Bayesian phylogenetic inference under mixed models. *Bioinformatics*, *19*, 1572–1574. https://doi.org/10.1093/bioinformatics/btg180

Ronquist, F., Teslenko, M., van der Mark, P., Ayres, D. L., Darling, A., Höhna, S., Larget, B., Liu, L., Suchard, M. A., & Huelsenbeck, J. P. (2012). MRBAYES 3.2: Efficient Bayesian phylogenetic inference and model

selection across a large model space. *Systematic Biology*, *61*, 539–542. https://doi.org/10.1093/sysbio/sys029

Schmidt, E. (1943). Bemerkungen über Lestiden. 2. Eine neue Gattung und Art aus Kamerun (*Eolestes diotima*). *Mitteilungen der Deutsche Entomologische Gesellschaft*, *11*, 102–111.

Selys-Longchamps, M. E. (1862). Synopsis des Agrionines. Troisième légion: *Podagrion. Bulletin de l'Académie royale de Belgique*, *14*, 5–44.

Sepkoski, J. J. Jr. (1996). Competition in macroevolution: The double wedge revisited. In D. Jablonski, D. H. Erwin, & J. H. Lipps (Eds.), *Evolutionary Paleobiology* (pp. 211–255). University of Chicago Press.

Simaika, J. P., Ware, J. L., Garrison, R. W., & Samways, M. J. (2020). Phylogeny of the Synlestidae (Odonata: Zygoptera), with an emphasis on *Chlorolestes* Selys and Ecchlorolestes Barnard. *Scientific Reports*, *10*, 1–12. https://doi.org/10.1038/s41598-020-72001-x

Sinitshenkova, N. D. (2003). Main ecological events in aquatic insects history. *Acta Zoologica Cracoviensia*, *46*, 381–392.

Suvorov, A., Scornavacca, C., Fujimoto, M. S., Bodily, P., Clement, M., Crandall, K. A., Whiting, M. F., Schrider, D. R., & Bybee, S. M. (2022). Deep ancestral introgression shapes evolutionary history of dragonflies and damselflies. *Systematic Biology*, *71*, 526–546. https://doi.org/10.1093/sysbio/syab063

To, P. Q., & Quang, T. V. (2018). A record of *Sinolestes editus* Needham, 1930 (Odonata: Zygoptera: Synlestidae) from the Central Highlands of Vietnam, with descriptions of the collected male and female specimens. *International Dragonfly Fund*, *124*, 1–9.

Vaidya, G., Lohman, D. J., & Meier, R. (2011). SequenceMatrix: Concatenation software for the fast assembly of multi-gene datasets with character set and codon information. *Cladistics*, *27*, 171–180. https://doi.org/10.1111/j.1096-0031.2010.00329.x

Vassilenko, D. V. (2005). New damselflies (Odonata: Synlestidae, Hemiphlebiidae) from the Mesozoic Transbaikalian locality of Chernovskie Kopi. *Paleontological Journal*, *39*, 280–283. https://doi.org/10.1134/S0031030118020041

Vassilenko, D. V. (2014). The first damselfly (Insecta: Odonata, Hemiphlebiidae) recorded from the Turonian of Israel. *Far Eastern Entomologist*, *278*, 1–7.

Wighton, D. C. (1980). New species of Tipulidae from the Paleocene of Central Alberta, Canada. *The Canadian Entomologist*, *112*, 621–628. https://doi.org/10.4039/Ent112621-6

Wighton, D. C. (1982). Middle Paleocene insect fossils from South-Central Alberta. *Proceedings of the 3rd North American Paleontological Convention*, *2*, 577–578.

Wighton, D. C., & Wilson, M. V. H. (1986). The Gomphaeschninae (Odonata: Aeshnidae): New fossil genus, reconstructed phylogeny, and geographical history. *Systematic Entomology*, *11*, 505–522. https://doi.org/10.1111/j.1365-3113.1986.tb00539.x

Wilson, M. V. H. (1996a). Insects near Eocene lakes of the Interior. In R. Ludvigsen (Ed.), *Life in stone: A natural history of British Columbia's Fossils* (pp. 225–233). University of British Columbia.

Wilson, M. V. H. (1996b). Taphonomy of a mass-death layer of fishes in the Paleocene Paskapoo Formation at Joffre Bridge, Alberta, Canada. *Canadian Journal of Earth Sciences*, *33*, 1487–1498. https://doi.org/10.1139/e96-112

Yu, X., & Xue, J. (2020). A review of the damselfly genus *Megalestes* Selys, 1862 (Insecta: Odonata: Zygoptera: Synlestidae) using integrative taxonomic methods. *Zootaxa*, *4851*, 245–270. https://doi.org/10.11646/zootaxa.4851.2.2

Zachos, J., Dickens, G., & Zeebe, R. (2008). An early Cenozoic perspective on greenhouse warming and carbon-cycle dynamics. *Nature*, *451*, 279–283. https://doi.org/10.1038/nature06588

Zheng, D. (2022). Odonatans in lowermost Cenomanian Kachin amber: Updated review and a new hemiphlebiid damselfly. *Cretaceous Research*, *118*, 104640. https://doi.org/10.1016/j.cretres.2020.104640

Zheng, D., Wang, B., Jarzembowski, E. A., Chang, S., & Nel, A. (2016). The first fossil Perilestidae (Odonata: Zygoptera) from mid-Cretaceous Burmese amber. *Cretaceous Research*, *65*, 199–205. https://doi.org/10.1016/j.cretres.2016.05.002